SPACECRAFT OBSERVATIONS OF THE SOLAR WIND COMPOSITION

S. J. Bame

An invited review

ABSTRACT

Solar wind composition studies by means of plasma analyzers carried on various spacecraft are reviewed. The average ratio of helium to hydrogen over the solar cycle is close to 0.045; values as low as 0.0025 and as high as 0.25 have been observed. High values have been observed following solar flares and interplanetary shock waves when the flare gas driving the shock arrives at the spacecraft. Ions of $^{3}He^{+2}$, $^{16}O^{+6}$, and $^{16}O^{+7}$ have been observed with Vela 3 electrostatic analyzers. Further measurements with Vela 5 analyzers have shown the presence of $^{14}N^{+6}$, $^{28}Si^{+7}$ to $^{28}Si^{+9}$, and $^{56}Fe^{+7}$ to $^{56}Fe^{+12}$ ions. The relative abundance of oxygen, silicon, and iron in the solar wind of July 6, 1969, was 1.00, 0.21, and 0.17, which is very similar to reported values for the corona. The ratio of helium to oxygen is variable; the average value of He/O is close to 100, but values between 30 and 400 have been observed.

INTRODUCTION

Continued expansion of the solar corona into interplanetary space forms the solar wind, which contains material recently a part of the outer convective zone of the sun. Photospheric matter is transported through the chromosphere into the million degree lower corona where the atoms are highly ionized. As the coronal density falls with increasing distance from the solar surface, interactions between particles decrease; at the same time the expansion velocity increases, and at relatively small distances from the sun the ionization state and composition become fixed, or "frozen in." For example, the ionization state of oxygen is expected to be virtually fixed at a heliocentric distance of about $1.5\,R_{\odot}$ and remain the same as the solar wind flows out beyond 1 AU [*Hundhausen et al.*, 1968]. Thus, observations of the solar wind elemental, isotopic, and ionic composition near earth can be used to deduce conditions deep within the corona and may contribute to a more complete understanding of how solar matter expands into interplanetary space. The reader is referred to recent papers of *Geiss et al.* [1970*a*], *Nakada* [1970], and *Hundhausen* [1970] and the references given by these authors for discussions of mechanisms that may control differentiation of the solar material as it expands outward through the lower levels of the solar atmosphere. The review of *Hundhausen* [1970] also provides a discussion of composition and other solar wind properties and references to earlier solar wind reviews.

In this paper, observations of the solar wind composition made with artificial spacecraft are described. The paper is divided into three major parts; the first part is concerned with the ions of the two most abundant nuclides in the sun—$^{1}H^{+}$ and $^{4}He^{+2}$. The second part reviews reported abundances of the universe, solar system, photosphere, chromosphere, and solar cosmic rays; the expected ionization state of the solar wind is considered, and a predicted energy per charge spectrum is presented. The last part discusses spacecraft observations of $^{3}He^{+2}$ and ions of the heavier elements ^{14}N, ^{16}O, ^{28}Si, and ^{56}Fe, and summarizes the present state of knowledge of the solar wind composition.

$^{1}H^{+}$ AND $^{4}He^{+2}$

The sun is known to be composed chiefly of normal hydrogen and helium. Almost no helium is ionized at the photospheric temperature of 6000° K, so conventional spectroscopic determinations of the photospheric helium abundance are not possible. Helium is observed in prominences, but an unambiguous determination of the

The author is at the University of California, Los Alamos Scientific Laboratory, Los Alamos, New Mexico.

solar helium content cannot be made from such measurements [*Unsöld*, 1969].

Three indirect methods have been used to estimate the helium abundance:

1. Models of stellar interiors predict a mass-luminosity relation that depends on the helium content of the star. For the sun helium-hydrogen ratios (by number) have ranged between 0.077 and 0.095 and have an average close to 0.09 [*Sears*, 1964; *Demarque and Percy*, 1964; *Weymann and Sears*, 1965; and *Morton*, 1968]. These values pertain to the solar interior and need not be representative of the photosphere.
2. The abundance of helium relative to other nuclei found in the solar cosmic rays has been found to be relatively constant from one energetic particle event to the next [*Gaustad*, 1964; *Biswas et al.*, 1966]. A relative solar helium abundance of 0.09 has been found by comparing the cosmic ray abundances of helium, carbon, nitrogen, and oxygen with the spectroscopic values of the photospheric abundances of hydrogen, carbon, nitrogen, and oxygen. Later determinations of 0.063 ± 0.015 have been made by *Lambert* [1967] and 0.062 ± 0.008 by *Durgaprasad et al.* [1968]. This method assumes that helium and other ions are accelerated nonpreferentially in the solar cosmic ray energization process, and pertains to the lower solar atmosphere.
3. *Iben* [1969] has used the upper limit of the solar neutrino flux established by *Davis et al.* [1968] to infer an upper limit of 0.049 to 0.064 for the helium-hydrogen abundance ratio, but again, the result pertains to the solar interior.

Thus, although the helium abundance of the photosphere of the sun is not known accurately, values up to 0.10 might be expected. The remainder of solar material is mostly hydrogen, since the total abundances of all elements heavier than helium are only a few tenths of a percent at most.

Solar Wind Average Relative Abundance of ^{4}He and ^{1}H

The detection of two groups of solar wind ions ascribed to $^1H^+$ and $^4He^{+2}$ has been reported by many observers, including *Snyder and Neugebauer* [1964], *Wolfe and Silva* [1965], *Coon* [1966], *Lazarus et al.* [1966], *Neugebauer and Snyder* [1966], *Wolfe et al.* [1966], *Hundhausen et al.* [1967], *Ogilvie et al.* [1968*a*], *Ogilvie and Wilkerson* [1969], *Robbins et al.* [1970], and *Formisano et al.* [1970]. The measured long-term average helium abundance is based on data from three spacecraft: Mariner 2, Vela 3, and Explorer 34. The results from these independent sources, which agree reasonably well, show that the solar wind helium abundance may be significantly lower than the solar abundance estimates discussed earlier.

Mariner 2 Observations. The Mariner 2 positive-ion curved plate electrostatic analyzer [*Snyder and Neugebauer*, 1964; *Neugebauer and Snyder*, 1966] accepted particles in a 6° square angular window centered near the solar direction. The positive ion flux was measured in a series of logarithmically spaced energy per charge channels. Spectra with a large peak and a smaller secondary peak were often observed; an example is shown in figure 1. Because of the predominance of hydrogen and helium in the sun, these peaks were attributed to $^1H^+$ and $^4He^{+2}$ ions traveling at a common mean speed, so the helium ions have four times the energy of the hydrogen ions and twice the energy per charge E/Q. Ions of $^4He^+$, which would appear at four times the E/Q of $^1H^+$, were not observed. Because of the large gaps between energy windows of the analyzer, accurate determinations could not be made of the flux peak widths. Consequently, these data were analyzed under the assumption that the $^4He^{+2}$ ions were four times as hot as the $^1H^+$ ions; this assumption gave better fits to the data than the assumption of equal temperatures and is supported by the results of *Robbins et al.* [1970], which show that the helium-hydrogen temperature ratios measured by Vela 3 very rarely have values near 1 but are much more likely to have values near 2.5 to 4.5 and sometimes higher.

From a total of 14,147 spectra measured between August 29 and December 30, 1962, 1213 spectra could be used in an analysis that yielded an average helium-hydrogen number ratio of 0.046. Most of these spectra

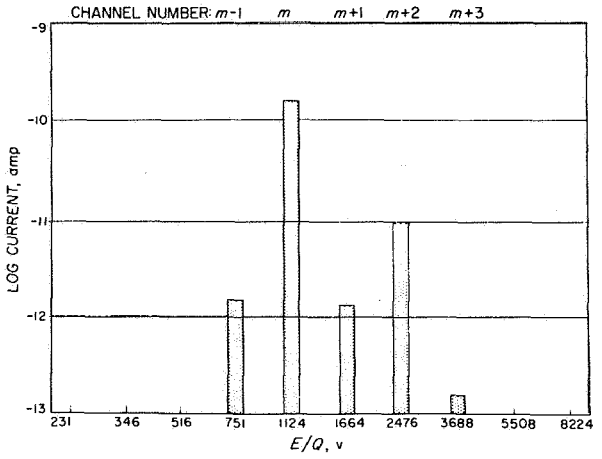

Figure 1. *Sample solar wind spectrum obtained by the Mariner 2 ion analyzer showing two groups presumed to be $^1H^+$ and $^4He^{+2}$ [Neugebauer and Snyder, 1966].*

were obtained when the solar wind speed was low, so there is some possibility of an observational bias in the derived ratio.

Vela 3 Observations. Hemispherical electrostatic analyzers using particle counting with electron multipliers [*Bame et al.*, 1967; *Gosling et al.*, 1967*a*; *Hundhausen et al.*, 1967] measured the positive ion flux in fan-shaped angular windows at eight different orientations of the two spinning Vela 3 spacecraft. Figure 2 shows a variety of spectra obtained that show two flux peaks attributable to $^1H^+$ and $^4He^{+2}$. This identification was strengthened by a pulse height analysis of the electron multiplier pulses in each peak (to be discussed later), which showed that the higher E/Q peaks are caused by ions of greater mass than those causing the lower peaks [*Bame et al.*, 1968*a*]. The energy window spacing of the Vela 3 analyzers permitted more complete definitions of the spectral peaks; this greater resolution coupled with the directional information made it possible to determine helium-hydrogen ratios without assumptions about the ion temperatures.

An analysis of the 1964 Vela 3 energy-angle data matrices obtained between July 24 and August 29, 1965, gave an average helium-hydrogen ratio of 0.042 [*Hundhausen et al.*, 1967]. More recently, *Robbins et al.* [1970] reported a value of 0.037 obtained from the analysis of 10,214 measurements made between July 1965 and July 1967. This later analysis also showed that the flow speed of the $^4He^{+2}$ ions is almost always the same as that of the $^1H^+$ ions.

Explorer 34 Observations. Particles were accepted into the Explorer 34 plasma detector [*Ogilvie et al.*, 1968*b*] in a fan-shaped angular window. Flux versus E/Q was measured in a single selected sector during a spacecraft rotation. In addition to the E/Q analysis, a crossed field velocity selector permitted a mass per charge separation of the ions with $M/Q = 1(^1H^+)$ and $M/Q = 2(^4He^{+2})$.

Figure 3 shows typical solar wind E/Q spectra at the separate M/Qs corresponding to hydrogen and helium. The Explorer 34 experiment essentially confirms the conventional identification of the two peaks. However, some ambiguity remains due to the fact that other ions with $M/Q = 2(^2H^+$ and fully ionized ^{12}C, ^{14}N, ^{16}O, etc.) and the same mean speed would also fall into the second peak. However, very little deuterium is expected in the modern sun, and the heavier elements fully ionized have very low abundances compared to helium as will be seen in the next section. An additional confirmation of the presence of ^4He is supplied by the mass spectrometer identification of ^4He in the aluminum foils exposed on the lunar surface by the Apollo astronauts [*Bühler et al.*, 1969; *Geiss et al.*, 1970*b*]. Considering the exposure times of the foils, the amount of helium captured was consistent with the assumption

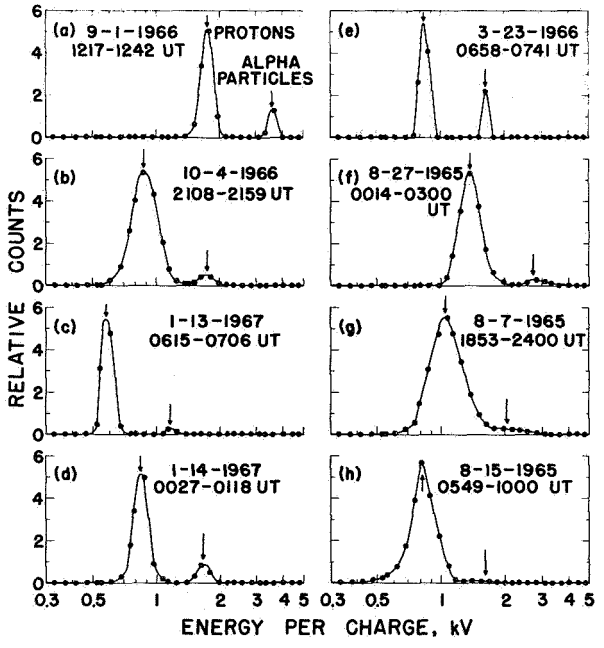

Figure 2. *Sample spectra from the Vela 3A and B analyzers. Two groups of ions, presumed to be $^1H^+$ and $^4He^{+2}$ are always observed in the solar wind. The second group was shown to have higher mass [Bame et al., 1968a].*

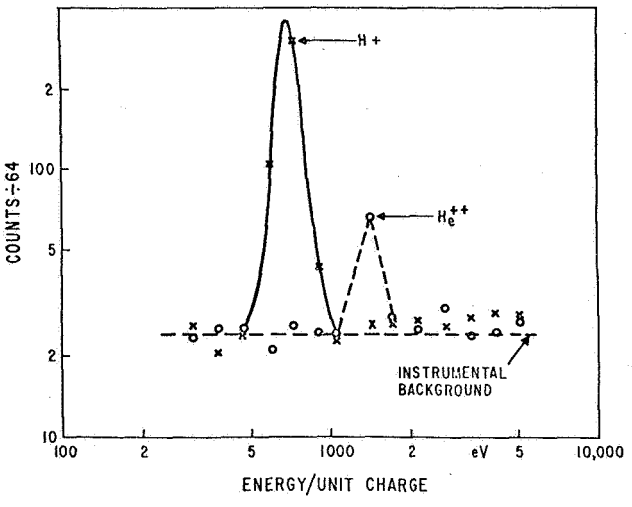

Figure 3. *Sample spectra from the Explorer 34 ion analyzer. The spectrum shown by the crosses is for $M/Q = 1$ ion ($^1H^+$); the spectrum shown by circles is for $M/Q = 2$ ions, presumed to be mainly $^4He^{+2}$ [Ogilvie et al., 1968a].*

that most of the second peak observed with spacecraft is $^4He^{+2}$.

Both the Vela 3 determination that the second group is higher mass and the Explorer 34 mass per charge separation eliminate the possibility that the peak ascribed to $^4He^{+2}$ is in actuality a nonthermal tail on the $^1H^+$ peak. The Explorer 34 channel spacing is similar to that in the Mariner 2 spectrum of figure 1, and an instrumental background produced by an on-board data processing system is present. Thus, under normal solar wind conditions, the observed $^4He^{+2}$ peak shows counts above background in only one or two channels, and determination of the helium abundance requires an assumption relating the $^4He^{+2}$ and $^1H^+$ temperatures.

The analysis of Explorer 34 data obtained between May 30, 1967, and January 1, 1968, has been reported by *Ogilvie and Wilkerson* [1969]. Under solar wind conditions such that the proton density is > 10 cm^{-3} and the $^4He^{+2}$ temperature is high enough that a three-point helium peak is obtained (and no assumption about temperature is necessary), the average helium abundance was found to be 0.051, in good agreement with the Mariner 2 and Vela 3 values.

Table 1, taken from *Hundhausen* [1970], summarizes the observations from these three sources. The agreement between the average values is satisfactory, particularly in view of the fact that there may be a solar cycle variation in the average value as discussed below. Note that the Mariner 2 value was obtained during the declining part of the last solar cycle, but before minimum. The higher value reported from Explorer 34 comes from a period farther from solar minimum than the Vela 3 value, and would appear to agree well with an extrapolation of the Vela 3 time history given in figure 7. Although measurements throughout a solar cycle would be desirable, the density number ratio seems to be well established at near 0.045.

Nearly all of the previously discussed indirectly derived values of the solar helium abundance are larger than the solar wind value of 0.045. As indicated earlier, some of the estimates are not necessarily representative of the outer layers of the sun. Possible effects of gravitational settling [*Parker*, 1963; *Geiss et al.*, 1970*a*; *Hundhausen*, 1970] also would permit differences in the solar photospheric and solar wind helium abundances.

Fluctuations in Solar Wind Helium Abundance

Substantial variations in the helium-hydrogen ratio have been reported by many observers, including *Coon* [1966], *Neugebauer and Snyder* [1966], *Hundhausen et al.* [1967], *Ogilvie et al.* [1968*a*], *Ogilvie and Wilkerson* [1969], and *Robbins et al.* [1970]. Figure 4 is the histogram from Explorer 34 presented by *Ogilvie and Wilkerson* [1969]. The histograms from Explorer 34 and Vela 3 are similar, and show a distinct skewing toward higher ratios. Values of the helium-hydrogen ratio have been observed with Vela 3 to range as low as 0.003 and

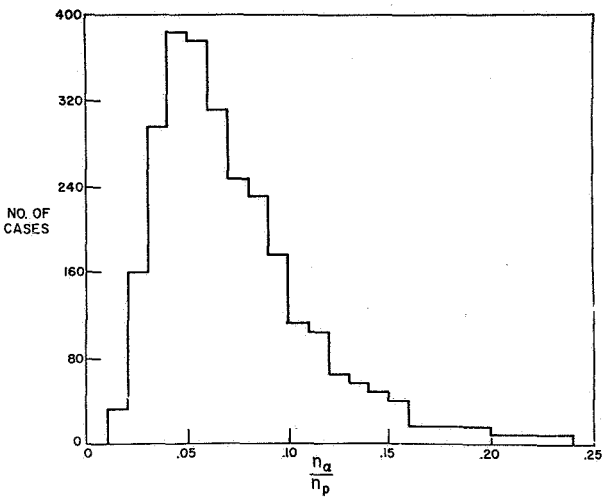

Figure 4. *Helium to hydrogen density ratio distribution observed by Explorer 34 between May 30, 1967 and January 1, 1968 [Ogilvie and Wilkerson, 1969].*

Table 1 *Observational determinations of the average relative abundance of helium and hydrogen in the solar wind*

Source	Period	⟨He/H⟩	Measurements	Comments
Mariner 2	Aug. 29 to Dec. 30, 1962	0.046	1,213	Energy-per-charge analysis only; assumptions about temperature; 10 percent of data included in analysis; sample favors low solar wind speeds
Vela 3	July 1965 to July 1967	0.037	10,314	Energy-per-charge analysis only; 60 percent of data included in analysis
Explorer 34	May 30, 1967 to Jan. 1, 1968	0.051	2,705	Energy-per-charge and mass analysis; 5 percent of data included in analysis; sample favors high solar wind density

as high as 0.25. Thus, the observations indicate that the helium abundance in the solar wind fluctuates over two orders of magnitude and that extremely high values are more common than would be expected if the abundances were distributed normally about the mean.

At times the helium abundance can remain at relatively high or low values for periods of many hours. An example from Vela 3 (fig. 5) shows that on September 3, 1966 the helium-hydrogen ratio remained above 7

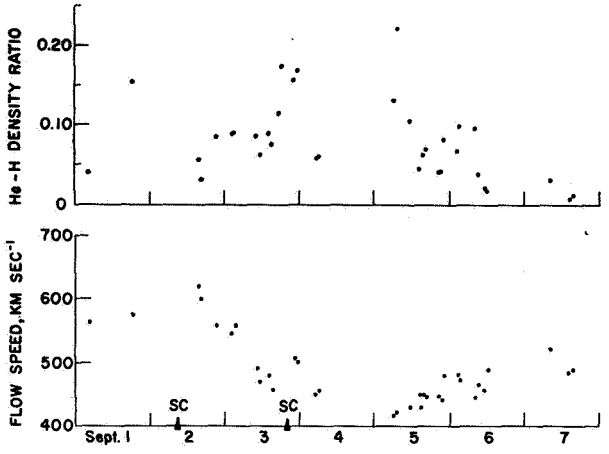

Figure 5. *Time history of Vela 3 helium to hydrogen density ratios and solar wind flow speed showing higher than average values of the helium abundance persisting throughout September 3, 1966. This was a time of high solar activity. Gaps in the data are caused by orbital positions out of the solar wind and times of no data transmission.*

percent most of the time over a period of a day. This was a time of considerable solar activity, which probably contributed to the high helium abundance, as discussed below.

An example of abnormally low abundance is given in figure 6. On December 10, 1965, the helium-hydrogen ratio remained in the 0.003-0.004 range for about 8 hr.

Further information about the helium abundance variations is gained by averaging the measurements over different time intervals. Figure 7 shows the helium-hydrogen number ratio, observed by Vela 3 satellites from July 1965, to June 28, 1967, averaged over both the 27-day solar rotation periods and over shorter 10-day periods. Averages over 27-day periods remove inhomogeneities that might exist in solar longitude and thus give the best spatial average over the entire solar corona that is possible with measurements made near the ecliptic plane. A small upward trend with time appears to be present in the 27-day averages. This trend appears

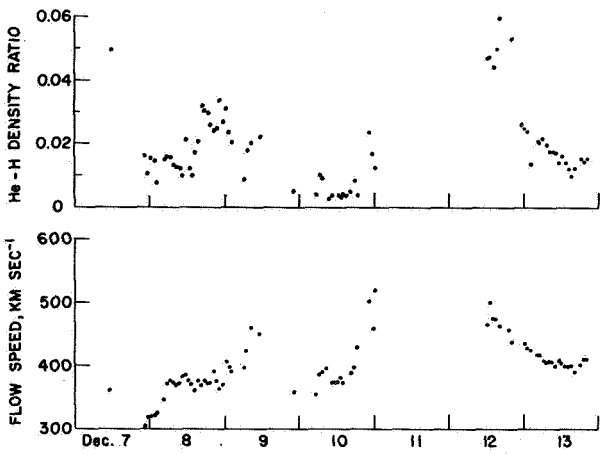

Figure 6. *Time history of Vela 3 helium to hydrogen density ratios and solar wind flow speeds showing a time of unusually low helium abundance (~0.003) persisting for 8 hr.*

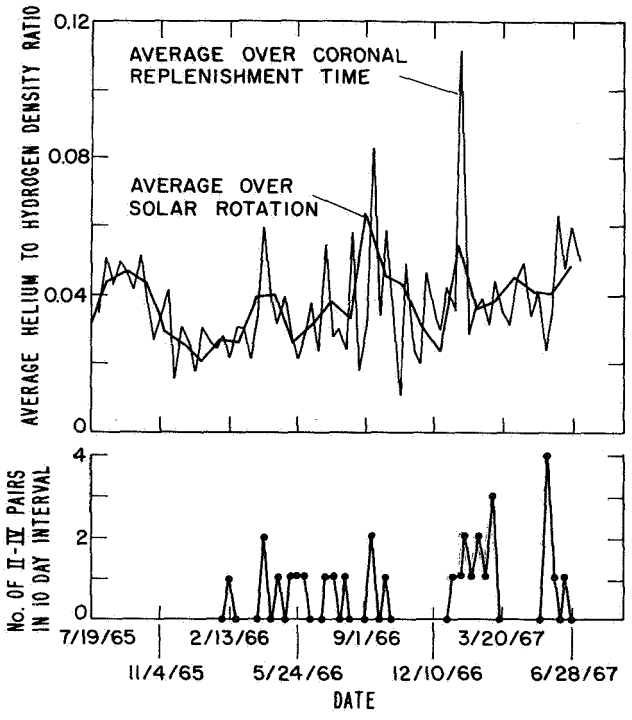

Figure 7. *Time variation of the helium to hydrogen density ratio from Vela 3A and B averaged over solar rotations and 10-day intervals [Robbins et al., 1970]. Also shown are the number of type II and type IV radio bursts in the corresponding 10-day intervals.*

to be real and is probably related to rising solar activity during this part of the solar cycle.

The 10-day averages show even larger fluctuations than the 27-day averages. Also plotted are the number of

pairs of type II and type IV radio noise bursts during the corresponding 10-day intervals. There appears to be a significant correlation between the occurrence of the radio noise bursts and peaks in the alpha abundance (*Hundhausen,* private communication). Such bursts are also known to be correlated with solar flares of large magnitude which often produce energetic particle events, interplanetary shock waves, and sudden commencements. Thus, again there seems to be a relationship between high helium content in the solar wind and solar activity.

Solar Wind Helium Abundance Enhancements

Evidence has been given suggesting that a high helium abundance in the solar wind seems to be directly related to solar flare activity. A number of observers have reported examples of a high helium content appearing 5 to 12 hr after an interplanetary shock or a geomagnetic sudden commencement. Table 2, taken from *Hirshberg et al.* [1970*a*], lists some of the reported events. For one of the events spectra obtained on January 13, 1967, before the interplanetary shock observation by Vela 3A and after the helium enhancement early on January 14, 1967, can be seen in figure 2. This helium enhancement apparently occurred at the time that the ATS 1 satellite observed a magnetopause crossing at 6.6 R_e [*Cummings and Coleman,* 1968]. The importance of the helium enhancement observed by Vela 3 [*Bame et al.,* 1968*b*] in providing the solar wind pressure required to push back the magnetopause has been pointed out by *Kavanagh et al.* [1970].

Spectra measured by Vela 3A on February 15 and 16, 1967, which show the passage of an interplanetary shock wave at 2345 UT on February 15 and the sudden helium enhancement on February 16, are shown in figure 8. The helium abundance was particularly low (0.01 to 0.02) both before and after the shock arrival. (No change is expected to occur in the helium abundance due to the passage of the shock, since the shock cannot change the composition of the ambient plasma through which it passes.) Nine hours after the shock passage the solar wind speed and density had increased beyond the postshock values, but the helium abundance was still low. The spacecraft was then engulfed in the magnetosheath by an outward movement of the bow shock and no further solar wind spectra were available until 0916 UT, after the bow shock had again moved behind the spacecraft. At this time a dramatic change had occurred in the helium abundance, but because of the wide spacing of energy channels available in the memory operating mode used at this time, exact values could not be determined. At 0940 UT a spectrum was obtained in the direct data transmission mode; in this mode many more energy channels are used and it is possible to compute a helium abundance of 0.22 for the 0940 UT spectrum. More complete descriptions of this event can be found in *Hirshberg et al.* [1970*a*] and *Hundhausen* [1970].

Further examples of helium enriched solar wind have been found in Vela 3 data obtained between July 1965 and July 1967 [*Hirshberg et al.,* 1970*b*]. Most of the strongest enhancements (He/H > 15 percent) followed major solar flares. During this period, 12 solar flares have been identified as probable sources of helium enrichment. An example is shown in figure 2(a), which shows a

Table 2 *Observations of helium-enriched interplanetary media discussed in the literature*

Percent helium	Date	Reference	Comments*
10–15	April 17, 1965	*Gosling et al.* [1967*b*]	Helium appears about 12 hr after an interplanetary shock was detected
12	July 11, 1966	*Lazarus and Binsack* [1969]	Helium associated with high velocity (≃ 700 km/sec) plasma
17	May 30, 1967	*Ogilvie et al.* [1968*a*]	Helium appears 5–1/2 hr after the sudden commencement of a geomagnetic storm; a class 3B flare occurred at 28°N, 33°W on May 28
18	January 14, 1967	*Bame et al.* [1968*b*]	Helium appears about 12 hr after an interplanetary shock was detected; a class 3B flare occurred on January 11, at 26°S, 47°W
22	February 16, 1967	*Hirshberg et al.* [1970*a*]	Helium appears about 9 hr after an interplanetary shock was detected; a class 4B flare occurred on February 13 at 20°N, 10°W

**Evidence suggesting that the enrichment was associated with a solar flare event.*

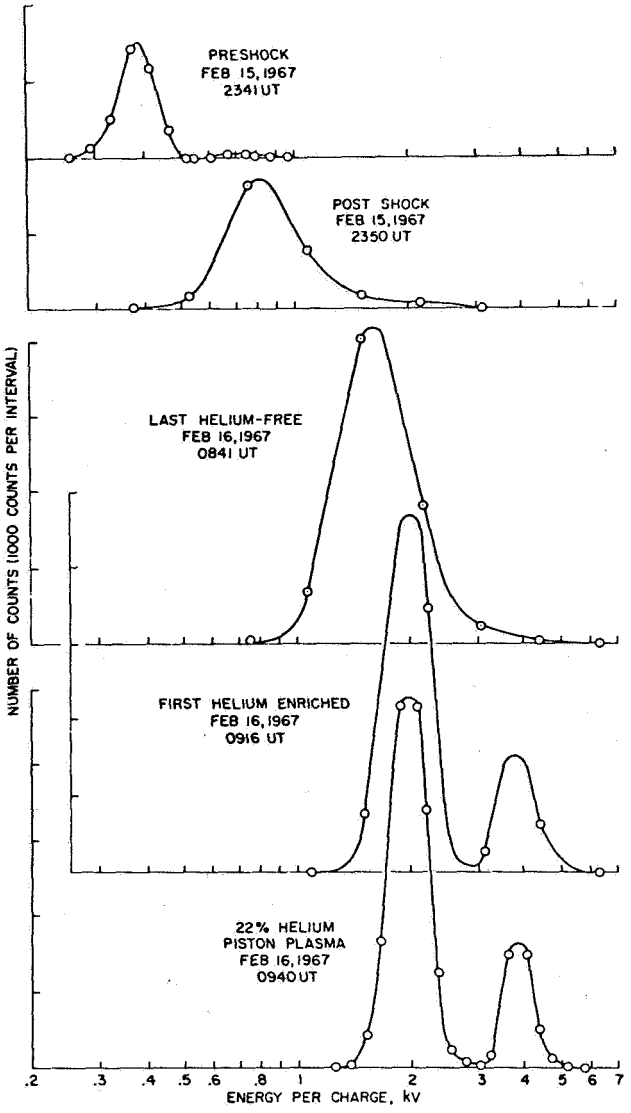

Figure 8. *Solar wind spectra observed by Vela 3A during the solar wind disturbance of February 15-16, 1967 [Hirshberg et al., 1970a].*

spectrum obtained at a time following numerous flares in late August.

It has been suggested by *Lazarus and Binsack* [1969] that a solar wind density and velocity increase observed at Pioneer 6 on July 10, 1966, following an interplanetary shock on July 9, might represent the arrival of plasma from the flare region—that is, the "driver gas." The events observed by Vela 3 and discussed previously seem to indicate that solar wind plasma with unusually high helium enrichment is ejected from flare regions lower in the solar atmosphere, where the coronal helium abundance is expected to be greater. Helium abundances near 0.20 are consistent with those predicted by the model of *Geiss et al.* [1970*a*] for the lower corona. There seems little doubt that the appearance of an enhanced alpha abundance after a flare signals the arrival of the flare region plasma driving the interplanetary shock preceding the enhancement [*Hirshberg et al.*, 1970*a*; *Bame et al.*, 1968*b*].

Unusually high enhancements following flares often last for relatively short times. For example, the 0.22 helium abundance for the February 15-16, 1967, event lasted for about 30 min. However, higher than average abundances have been observed to persist for many hours (fig. 5), and such times of high abundance can usually be associated with solar activity. Another time of helium enhancement produced the spectrum seen in figure 2(e). This event has been discussed by *Bame et al.* [1968*a*], who showed that in addition to a helium enhancement, heavier ions were observable in the solar wind at this time. *Hundhausen et al.* [1968] and *Hundhausen* [1970] have shown that this solar wind stream can plausibly be associated with a single large plage area crossing the solar disk. The heavier ion abundances suggested that the stream began in a coronal region with temperatures higher than normal, as might be expected above a plage region.

Abrupt decreases, as well as increases, may be expected in the helium abundance, as the solar wind stream passing the earth changes from a coronal source region above an active area to a source region above a quiet area. An example of such an event is seen in figure 9. The upper spectrum contained a high helium abundance. This spectrum also contained observable amounts of ^{3}He and ^{16}O ions [*Bame et al.*, 1968*a*], which cannot be seen here because of the linear ordinate. Eight hours later another spectrum measurement showed that, although the solar wind speed and temperature were still about the same, the helium abundance had dropped from >0.10 to about 0.005. Other sudden appearances of increased and decreased helium abundance, which show the stream-like character of the solar wind, can be found in figures 5 and 6.

ION SPECIES THAT MIGHT BE OBSERVABLE IN THE SOLAR WIND

Since the sun contains small quantities of elements and isotopes other than normal hydrogen and helium, it might be expected that other ions should be present in the solar wind. Indeed, the model of *Geiss et al.* [1970*a*] shows that if $^{4}He^{+2}$ is observed in the solar wind, ions of other elements as heavy as iron should also be caught up by the expanding corona and carried along in the solar wind. In the preceding section, measurements showing that the solar wind always contains $^{4}He^{+2}$ were reviewed, and it seems reasonable that other solar

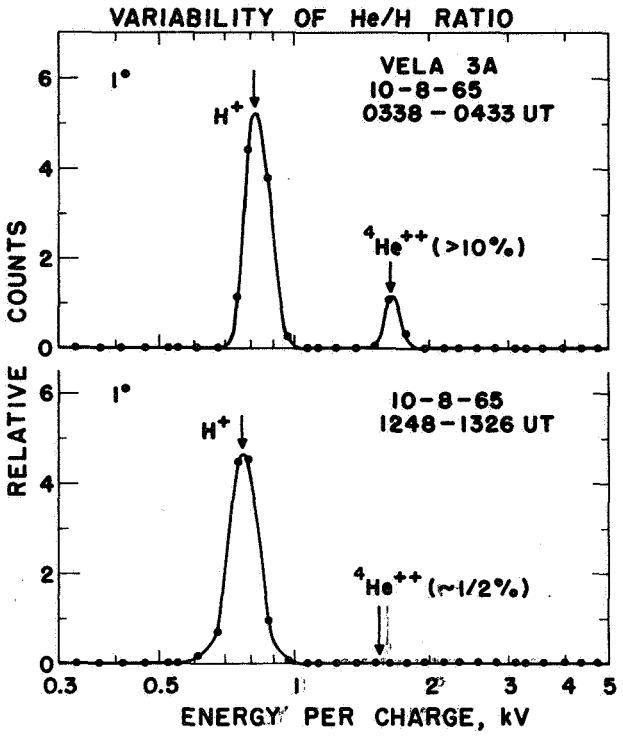

Figure 9. *Solar wind spectra from Vela 3A showing a sudden decrease in the helium abundance.*

materials should also be present, although probably in varying amounts compared to $^{1}H^{+}$.

Relative Abundances

Relative abundances of the more common nuclides normalized to oxygen are given in table 3. It might be argued that the abundances of the corona are most closely associated with the solar wind abundances, since the solar wind is an extension of the corona into interplanetary space. Inspection of the table shows some striking differences in photospheric, coronal, and solar cosmic ray abundances, particularly for nuclides above ^{20}Ne except for ^{32}S.

Oxygen, carbon, and nitrogen are likely candidates for observation with a sufficiently sensitive and appropriately designed solar wind experiment. If the coronal abundances are most nearly related to solar wind abundances, the other elements listed in the coronal abundance column, with the possible exception of ^{32}S, are also prime candidates for detection.

The possibility that solar wind abundances may be closely related to coronal abundances has been strengthened by the results of *Pecker and Pottasch* [1969]. These authors show that the chromospheric iron abundance is the same as the coronal iron abundance, and conclude that the coronal and chromospheric abundances are not significantly different. They also conclude that the differences between the chromospheric and photospheric abundances given by *Goldberg et al.* [1960] are significant, especially in the case of iron, and that the differences may be due to both departures in local thermodynamic equilibrium not taken into account, and the use of poorly determined f values to obtain the photospheric abundances. The abundances given by *Unsöld* [1969] and shown in table 3 also show large differences from those of the corona, especially in the case of ^{56}Fe.

New calculations for the magnetic dipole transition probabilities of [Fe II] lines by *Nussbaumer and Swings* [1970] have led these authors to a redetermination of the photospheric iron abundance. They conclude that

Table 3 *Relative abundances of the more common nuclides normalized to oxygen*

Nuclide	Cosmic *Allen* [1963]	Solar system *Cameron* [1968]	Photosphere *Unsöld* [1969]	Corona (UV lines) *Pottasch* [1967]	Solar cosmic rays *Biswas et al.* [1966]
^{1}H	1480	1100	1700	--	varies
^{3}He	--	0.03	--	--	--
^{4}He	214	90	--	--	107
^{12}C	0.45	0.56	0.60	2.00	0.59
^{14}N	0.14	0.10	0.15	0.24	0.19
^{16}O	1.00	1.00	1.00	1.00	1.00
^{20}Ne	0.41	0.09	0.11	0.14	0.13
^{24}Mg	0.04	0.04	0.05	0.12	0.04
^{28}Si	0.04	0.04	0.05	0.20	0.03
^{32}S	0.03	0.02	0.03	0.08	--
^{56}Fe	0.01	0.04	0.006*	0.20	$\leqslant$0.02*

**Newer values of these abundances are discussed in the text.*

the iron abundance is in agreement with the abundance for the meteorites, corona, and chromosphere, as shown in table 4.

Much attention has been devoted to the coronal iron abundance. Measurements made by *Malville and Schmahl* [1968] during the eclipse of November 1966 have shown that the high abundance persists out to at least $1.75\,R_\odot$. *Pottasch* [1964] analyzed the 1952 eclipse observations of *Fedoretz and Ezerskii* [1953], made out to $2\,R_\odot$, and showed that the high iron abundance persisted to that height. Thus, iron seems likely to be present in the solar wind.

The attention devoted to the abundance of iron is partly due to the intensity and uniqueness of its optical spectrum from the corona. If equal attention were devoted to measurements of the photospheric and coronal lines of silicon, for example, it seems reasonable to suppose that some of the silicon abundance discrepancy seen in table 3 might be resolved also. Thus, at the present time it is not clear that there are any large differences in the abundances of the heavier elements in the photosphere, chromosphere, and corona.

The abundance of the iron-group nuclei relative to oxygen in the September 2, 1966, solar cosmic ray event has been reported as 0.011 ± 0.003 by *Bertsch et al.* [1969], who believe that most of the measured nuclei were ^{56}Fe. They conclude that the measured relative abundance is easily consistent with the lower values of the photospheric iron abundance discussed earlier in this section. If in fact the higher values given by *Nussbaumer and Swings* [1970] are more nearly correct, the result of Bertsch *et al.*, may imply a less efficient acceleration of the heavier nuclei in the solar cosmic rays. The standard assumption that the photospheric and solar cosmic ray abundances of helium and heavier elements are the same would then be in doubt, and the photospheric helium abundance discussed earlier may actually be slightly smaller than the quoted values.

Ionization State of Solar Wind Constituents

It has been recognized for some years that the lower corona is very hot, having temperatures in the million-degree range. Hydrogen atoms coming from the photosphere are expected to become ionized as they expand into the corona. Helium is expected to become fully ionized; almost no $^4He^+$ ions are expected to exist in the corona at a temperature of $1X10^{6\,\circ}K$ [*Tucker and Gould,* 1966]. The existence of the two prominent ion species $^1H^+$ and $^4He^{+2}$ reviewed earlier confirm these expectations.

After hydrogen and helium, oxygen is one of the most abundant elements in the corona. In the corona the most abundant oxygen ions are expected to be $^{16}O^{+6}$ and $^{16}O^{+7}$ at temperatures between $1X10^{6\,\circ}K$ and $2X10^{6\,\circ}K$ [*Tucker and Gould,* 1966; *Allen and Dupree,* 1969; *C. Jordon,* 1969].

The ionization state of oxygen in the expanding corona has been considered by *Hundhausen et al.* [1968], for the ions $^{16}O^{+5}$ to $^{16}O^{+8}$. Collisional ionization was taken to be the dominant process for raising the ionization level, while radiative and dielectronic recombination were taken to be the dominant processes for reducing the level. The ionization rates of *Tucker and Gould* [1966] were used in the coronal-solar wind model of *Whang and Chang* [1965]. It was shown

Table 4 *Comparison of solar iron abundances*

Solar layer	$\log N_{Fe}$ (where $\log N_H = 12.0$)	Reference
Corona	from 7.3 to 7.7	*Jordan* [1966], *Pottasch* [1968], *Widing and Sandlin* [1968], *Nikolski* [1969]
Chromosphere	7.7	*Pecker and Pottasch* [1969]
Meteorites	7.5	*Urey* [1967]
Cosmic rays	7.0 to 7.2	*Bertsch et al.* [1969]
Photosphere	6.6 from Fe I and Fe II*	*Grevesse* [1969]
	7.5 from [Fe II]	*Grevesse and Swings* [1969]
	7.6 from Fe I and Fe II	*Garz et al.* [1969*a,b*], *Bascheck et al.* [1970]
	7.2 from Fe I	*Ross* [1970]
	7.5 from [Fe II] (magnetic dipole)	*Nussbaumer and Swings* [1970]

**This value is a mean of all the usually admitted photospheric iron abundances from permitted lines obtained between 1960 and 1969, including the often-cited value 6.66 of Goldberg et al. [1960]. Not included were the more recent values of Withbroe [1969], $\log N_{Fe} = 6.80$; and Rogerson [1969], $\log N_{Fe} = 6.85$.*

that processes that change the ionization state become less probable as a parcel of coronal plasma expands away from the sun, due to the increase in the ionization and recombination times as the plasma becomes more tenuous. At the same time the expansion scale time decreases rapidly so that at relatively small heights above the solar surface, the ionization state is very nearly fixed, or "frozen-in." The results of this analysis for a base coronal temperature of 1.58×10^6 °K are shown in figure 10 by the solid curves. The dashed curves show the state if the static solutions are assumed. The ionization state for the dynamic solution is frozen in at about 1.5 $R_\odot$ and should not change appreciably out to 1 AU. Thus, the ionization state observed near earth is representative of conditions deep within the corona.

The state of ionization of the solar wind oxygen as a function of temperature, derived from this analysis, is shown in figure 11. At temperatures between 1×10^6 and 2×10^6 °K, $^{16}O^{+6}$ is the most abundant. Around 2×10^6 °K, $^{16}O^{+7}$ reaches a maximum abundance due to the decreasing $^{16}O^{+6}$ and increasing $^{16}O^{+8}$. At 3×10^6 °K, the major fraction of solar wind oxygen would be in $^{16}O^{+8}$, which has an M/Q value of about 2.0, so that it would fall in the same group with $^4He^{+2}$ in an E/Q spectral analysis. Note that even at 1×10^6 °K the abundance of $^{16}O^{+5}$ is very low.

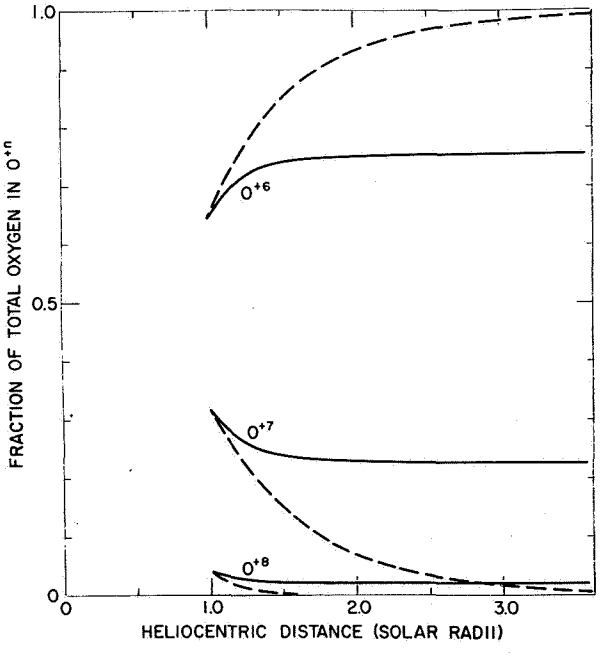

Figure 10. *The oxygen ionization state in the expanding corona (solid lines) and in a static corona (dashed lines), for a base temperature of 1.58×10^6 °K [Hundhausen et al., 1968].*

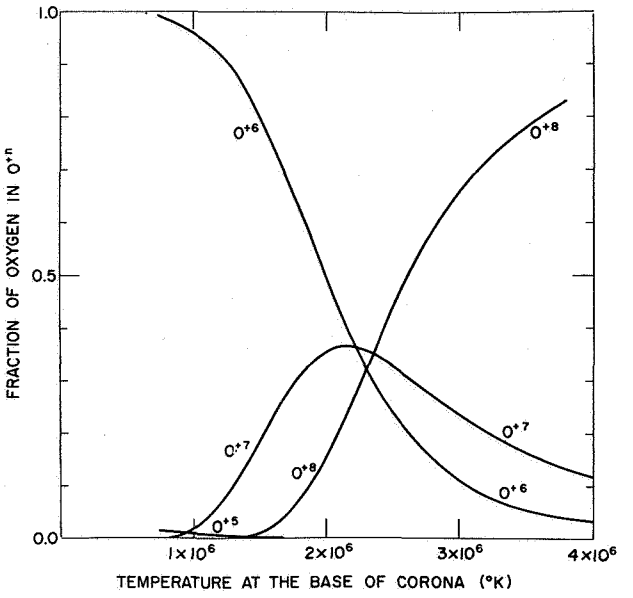

Figure 11. *The oxygen ionization state at large heliocentric distances as a function of temperature at the base of the corona [Hundhausen et al., 1968].*

Similar calculations have been carried out for ^{12}C by *Hundhausen et al.* [1968]. For a coronal base temperature of 1.58×10^6 °K, the frozen-in state has 96 percent of the carbon in the form of $^{12}C^{+6}$—that is, fully ionized—and the remaining 4 percent in the form of $^{12}C^{+5}$.

This ionization state analysis for an expanding corona has not been carried out for the heavier elements such as neon, magnesium, silicon and iron. Recent ionization equilibrium calculations of *Cox and Tucker* [1969], *Jordan* [1969], and *Allen and Dupree* [1969] can be used to estimate the ionization states of the elements as a function of the coronal temperatures where the states become frozen in the expanding plasma. To illustrate what may be expected for ^{56}Fe, ionization state envelopes taken from Allen and Dupree for four temperatures are shown in figure 12. The distribution of iron ions is quite sensitive to temperature and presumably measurements of such distributions in the solar wind could provide coronal temperatures with some precision. However, the accuracy with which this technique might be used is partly limited by the accuracy of the ionization equilibrium calculations. Significant differences can be noted in the calculations made by various authors.

Predictions of the Solar Wind Composition and Ionization State

Several predictions of the E/Q spectrum of the solar wind have been published, using various values for the

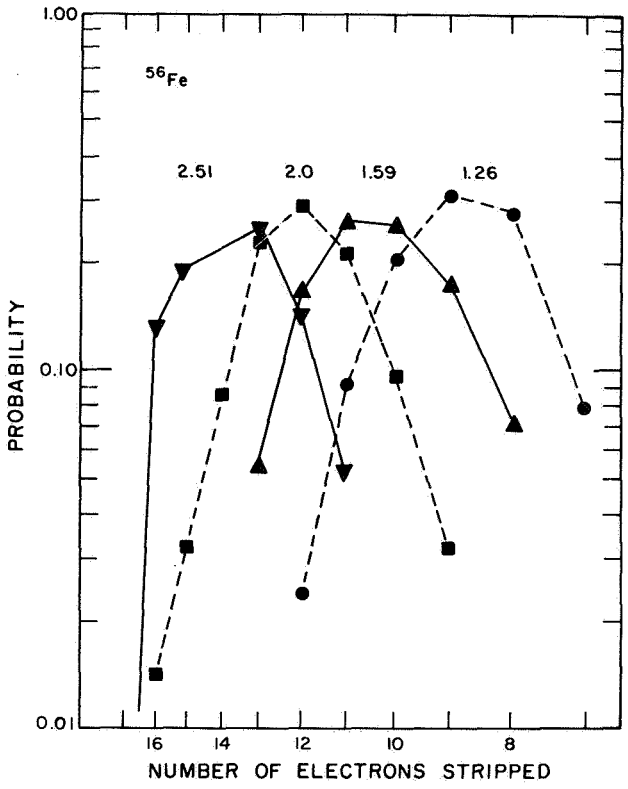

Figure 12. *Ionization state envelopes of ^{56}Fe for different coronal temperatures, in units of 10^6 °K, taken from the ionization equilibrium calculations of Allen and Dupree [1969].*

composition and various ionization state determinations. The predictions have assumed that all ion species have the same mean velocity. This assumption has been proven valid experimentally as shown later. The model of *Geiss et al.* [1970*a*] also predicts the same velocities if the $^1H^+$ and $^4He^{+2}$ velocities are the same. *Lange and Scherb* [1970] have shown spectra calculated using the *Cox and Tucker* [1969] ionization state values for a static corona with $T = 1.5 \times 10^6$ °K. Spectra for three assumed sets of oxygen, carbon, nitrogen, neon, magnesium, and silicon abundances relative to that of helium are given and compared with Vela 3 experimental determinations made by *Bame et al.* [1968*a*]. Lange and Scherb show that silicon ion species may produce resoluable peaks in a solar wind E/Q spectrum.

Similar predictions have been made by *Holzer and Axford* [1970*a*], who used the solar system abundances given by *Cameron* [1968] and shown in table 3, and the ionization equilibrium calculations of *Jordan* [1969] for $T = 1.26 \times 10^6$ °K. The resulting spectra were again compared with the data from Vela 3. Holzer and Axford concluded that both silicon and iron ion species may produce resolvable peaks.

Another prediction has been given by *Bame et al.* [1970] and will be discussed here in some detail. The coronal abundances given by *Pottasch* [1967] were assumed to be the same for the solar wind for elements above helium. Table 5 gives the predicted solar wind ion

Table 5 *Predicted solar wind ion species assuming Pottasch coronal abundances, a static corona ionization state for 1.5×10^6 °K, and $V = 440$ km sec^{-1}*

Ion species	E/Q	Species fraction	Coronal abundance	Species abundance	Ion species	E/Q	Species fraction	Coronal abundance	Species abundance
$^1H^+$	1.00	1.00	--	--	Mg^{+8}	2.98	0.01		0.001
$^2H^+$	2.00	1.00	--	--	Mg^{+9}	2.64	0.15	0.12	0.02
$^3H^+$	3.00	1.00	--	--	Mg^{+10}	2.38	0.70		0.08
$^3He^{+2}$	1.50	1.00	--	--	Si^{+7}	3.97	0.11		0.02
$^4He^{+2}$	1.99	1.00	--	--	Si^{+8}	3.47	0.34	0.20	0.07
C^{+5}	2.38	0.15	2.00	0.30	Si^{+9}	3.08	0.36		0.07
C^{+6}	1.99	0.85		1.70	Si^{+10}	2.78	0.13		0.03
N^{+5}	2.78	0.20		0.05	S^{+8}	4.00	0.11		0.01
N^{+6}	2.32	0.60	0.24	0.14	S^{+9}	3.53	0.35	0.08	0.03
N^{+7}	1.99	0.20		0.05	S^{+10}	3.17	0.35		0.03
O^{+6}	2.65	0.83	1.00	0.83	Fe^{+8}	6.94	0.06		0.01
O^{+7}	2.27	0.17		0.17	Fe^{+9}	6.17	0.20		0.04
Ne^{+8}	2.48	0.98	0.14	0.14	Fe^{+10}	5.55	0.26	0.20	0.05
					Fe^{+11}	5.05	0.25		0.05
					Fe^{+12}	4.63	0.13		0.03
					Fe^{+13}	4.27	0.04		0.008

species abundances for a static corona ionization state at $1.5X10^{6}$°K. Included in the table are the energy per charge values at which the various ion species are expected if the $^{1}H^{+}$ E/Q value is 1.00 and all species have the same velocity. For these assumptions, ion species positions should be M/M_pQ, where M is the ion mass, Q the ion charge, and M_p the proton mass. At proton energies other than 1.00, the same E/Q ratios are expected.

Ionization state calculations of *Cox and Tucker* [1969] were used for carbon, nitrogen and magnesium, those of *Allen and Dupree* [1969] for oxygen, neon, silicon, and iron, and those of *Jordan* [1969] for sulfur. The fractions of the various ion species expected, as shown in the table, were multiplied by the coronal abundances to obtain the species abundances.

Inspection of the table 5 species abundances and expected E/Q positions reveals a number of interesting features. The most abundant resolvable ions other than $^{1}H^{+}$ and $^{4}He^{+2}$ should be $^{16}O^{+6}$ for a coronal temperature of $1.5X10^{6}$°K. Some species lie very close together such as $^{12}C^{+5}$, $^{14}N^{+6}$, $^{16}O^{+7}$, and $^{24}Mg^{+10}$, but of these the carbon and oxygen species are expected to be more abundant than the others. The ion species of ^{24}Mg and ^{32}S are not as abundant as those of ^{28}Si and ^{56}Fe. Some of the silicon and all of the iron ion species E/Q positions listed are well separated from the species of the lighter elements.

Using the results of table 5, a predicted spectrum was synthesized as follows. The $^{4}He^{+2}$ peak from a particular solar wind spectrum measured on Vela 5A was used. Each of the ion species above $^{4}He^{+2}$ was assumed to produce in the electrostatic analyzer 6 percent wide at half maximum gaussian peaks. The heights of the peaks are proportional to the ion species abundances. This synthesized spectrum was joined onto the helium high-energy tail in a special way, as described in the next section. The resulting spectrum is shown in figure 13. For simplicity, the hydrogen peak is omitted here. A second prediction using solar system abundances is also shown by the dashed groups which lie considerably lower. Use of the older photospheric abundance of iron given in table 3 would drop the iron lines off the graph.

Table 5 and figure 13 show that sulfur and magnesium lines are hidden below the more prominent lines. The $^{16}O^{+7}$ line is hidden in the $^{4}He^{+2}$ tail. A partly resolved line due to $^{12}C^{+5}$ appears between $^{4}He^{+2}$ and $^{16}O^{+6}$. Other lines below $^{16}O^{+6}$, such as $^{20}Ne^{+8}$ and $^{14}N^{+6}$, are also hidden.

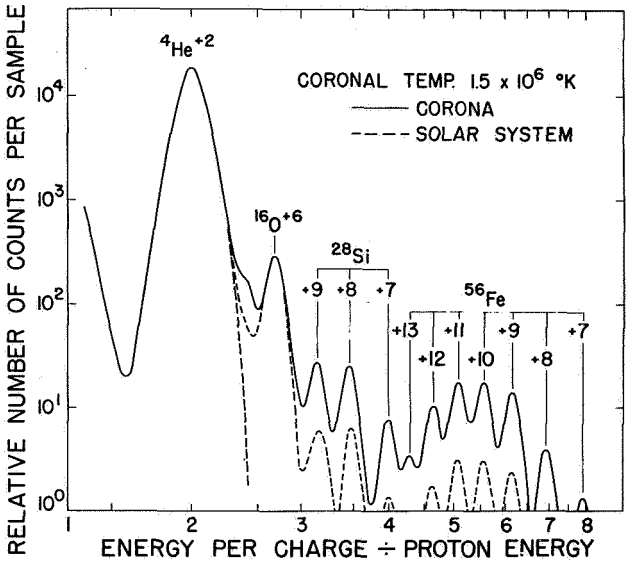

Figure 13. *A predicted solar wind spectrum as it would be observed with a suitable electrostatic analyzer. The $^{1}H^{+}$ peak is not shown. Relative peak heights of ion species above $^{4}He^{+2}$ are taken from table 5.*

SPACECRAFT OBSERVATIONS OF ^{16}O, ^{3}He, ^{28}Si, AND ^{56}Fe ION SPECIES

The first observations of ion species other than $^{1}H^{+}$ and $^{4}He^{+2}$ were made with electrostatic analyzers on the two Vela 3 spacecraft [*Bame et al.*, 1968*a*]. Further observations are being made on the two pairs of earth-oriented satellites Vela 5A and B, and Vela 6A and B with improved instrumentation. A report of Vela 5A results has been given by *Bame et al.* [1970]. No other spacecraft instrument measurements of resolved ion species other than $^{1}H^{+}$ and $^{4}He^{+2}$ are known to the author. Measurements of some of the solar wind noble gas nuclides trapped in aluminum foils exposed on the lunar surface by the Apollo 11 and 12 astronauts have been reported by *Bühler et al.* [1969] and *Geiss et al.* [1970*b*].

Vela 3 Instrument Details

Each of the two spin-stabilized Vela 3 satellites carried a hemispherical electrostatic analyzer. Some general details of the instruments, orbits, and methods of analyzing the solar wind data have been given by *Gosling et al.* [1967*a*], *Hundhausen et al.* [1967], and *Bame et al.* [1967]. Additional details are needed for a discussion of the ion species measurements.

Special conditions are necessary for the ion species to be resolved. With Vela 3 analyzers the efficiency and cycle times require that the solar wind conditions remain rather constant for periods of around 20 to 30 min in order to collect sufficient numbers of counts to resolve

the ion species. The solar wind $^1H^+$ and $^4He^{+2}$ temperatures must be low, as well as those of other species, to permit resolution of the groups. The instrumental resolution must be high enough and E/Q level spacings close enough to resolve the closely spaced groups.

With Vela 3 these conditions are met part of the time, although it will be seen that the E/Q level spacings are marginal. The electrostatic analyzer intrinsic E/Q resolution is about 2.8 percent and level spacing is about 11 percent. Fixed voltage levels exercised in a 4 minute cycle are used on Vela 3A and B, so significant gaps exist between E/Q windows. Particles are accepted in a fan-shaped solid angle of approximately 3° in spacecraft longitude and 100° in latitude. The spin-stabilized spacecraft sweep the acceptance angle past the sun two times per second, while counting in intervals of 8 msec triggered by the sun in such a way that flux measurements are made in eight angular ranges. Five of these angular ranges are centered at angles of −11°, −5°, 1°, 7°, and 14° from the solar direction. Usually the majority of counts from solar wind ions are observed in two or three angular ranges when temperatures are low enough for resolution of ion species.

Analyzed ions enter an electron multiplier and produce secondary electrons. The number of electrons produced is highly dependent on the ion mass for equal ion speeds. The electron multiplier pulses are amplified and counted above three charge threshold levels *A*, *B*, and *C*, which have relative sensitivities of 60, 6, and 1. Most of the ions are counted at level *A*, independent of their mass. Significant losses in counting protons and small losses for helium ions occur at level *B*. At level *C*, protons and helium ions are counted with much less efficiency than heavy ions. This feature helps in identifying heavy ions and in separating them from the high energy tail of the $^4He^{+2}$ distribution.

At any given time, simultaneous counts from levels *A* and *B* or levels *A* and *C* are transmitted to the ground. The choice is made by command.

Vela 3 Solar Wind Heavy Ion Spectra

A spectrum demonstrating the presence of $^{16}O^{+6}$ ions is given in figure 14. At this time the counts at levels *A* and *B* were transmitted. Counts measured at angles of −5° and 1° in four data cycles between 1226 UT and 1243 UT were summed at each of the E/Q levels to form the spectra. The two peaks attributable to $^1H^+$ and $^4He^{+2}$, always seen in Vela 3 spectra, are present. A third peak, present on the high energy $^4He^{+2}$ tail, is caused by ions heavier than $^4He^{+2}$; at level *B*, these ions are more efficiently counted than $^4He^{+2}$. Arrows are shown at positions where $^{16}O^{+7}$ and $^{16}O^{+6}$ ions would

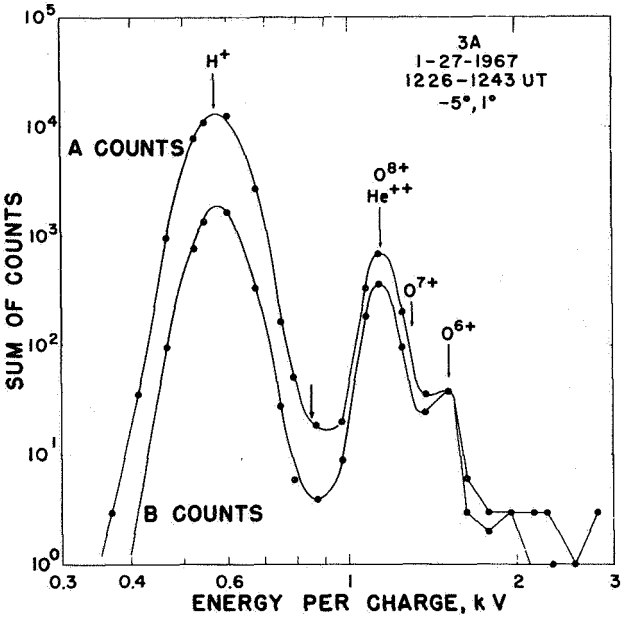

Figure 14. *Solar wind spectra from Vela 3A obtained simultaneously at two different sensitivity levels. A third ion species attributed to $^{16}O^{+6}$ is present, as well as other unresolved species.*

be expected, based on the observed positions of the lighter ions. That $^{16}O^{+6}$ ions are present in the spectrum is well established, but it is clear that other ion species such as $^{16}O^{+7}$, $^{12}C^{+5}$, $^{14}N^{+7}$, and $^{20}Ne^{+8}$ could also be present but unresolved in this spectrum (compare the predicted spectrum of figure 13 and table 5). Counts at E/Q values above $^{16}O^{+6}$ are partly background and partly unresolved heavier ions.

At the time that this spectrum was measured oxygen appears to have been particularly abundant. If allowance is made for other species, the He/O ratio is still rather small and may have a value near 30. The precision with which this ratio can be determined is not very great, of course. The ratio He/O as observed in a number of Vela 3 spectra is variable; the highest ratio measured is ~400.

One of the spectra published in *Bame et al.* [1968*a*] is shown in figure 15. The spacecraft was transmitting *A* and *C* level counts at this time. Counts from angles −5° and 1° were summed for four data cycles between 0388 and 0355 UT. One count was added at each E/Q level to show level positions where the counts were zero. Based on the $^1H^+$ and $^4He^{+2}$ positions, arrows show where various ion species would be found if present. The arrows for oxygen ions at higher E/Q than $^{16}O^{+5}$ are intended to give the E/Q scale and do not imply that those ions were present [*Bame et al.*, 1968*a*].

A peak at an E/Q position 1.5 times higher than $^1H^+$

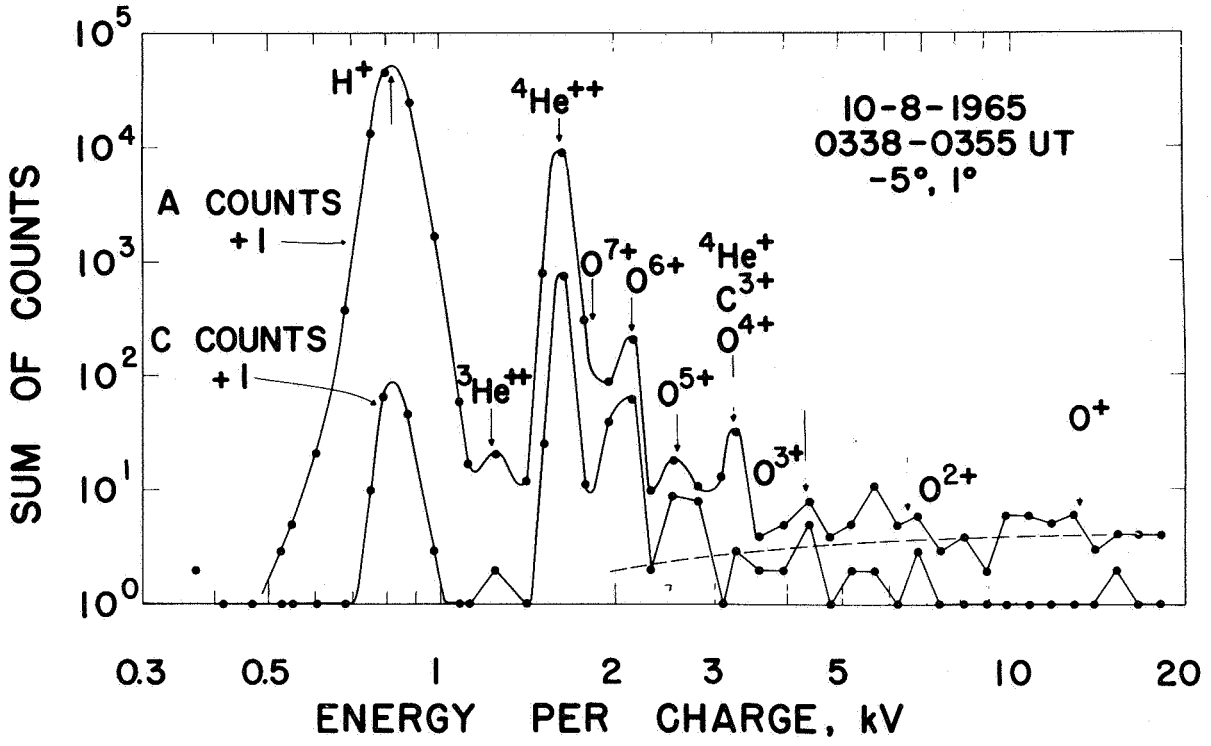

Figure 15. *Solar wind spectra from Vela 3A obtained simultaneously at two different sensitivity levels. This spectrum was interpreted by Bame et al. [1968a] to show the presence of* $^{3}He^{+2}$, $^{16}O^{+6}$, $^{16}O^{+5}$, *and* $^{4}He^{+}$ *ions, as well as other unresolved species. A new interpretation based on later Vela results eliminates the* $^{16}O^{+5}$ *identification. (See fig. 19.)*

appeared in this spectrum and a companion spectrum a little later. This can only correspond to $^{3}He^{+2}$, showing that ^{3}He exists in the modern sun. The solar wind ^{3}He abundance at this time was $\sim 10^{-3}$ that of ^{4}He. At another time when the ion temperatures were very low and ^{3}He would have been resolved if sufficiently abundant, upper limits of 2×10^{-4} and 4×10^{-4} were set. In other examples the $^{3}He/^{4}He$ ratio was higher than 10^{-3} but the $^{1}H^{+}$ and $^{4}He^{+2}$ tails prevented accurate determinations. Thus, the spacecraft observations indicate a variable abundance of ^{3}He relative to ^{4}He in the solar wind. A similar conclusion has been reached by *Geiss et al.* [1970*b*] from the Apollo foil experiments.

Again, the $^{16}O^{+6}$ group is quite prominent; the *C*-count spectrum shows $^{16}O^{+7}$ to be less abundant. In some other examples, with the E/Q levels appropriately placed, $^{16}O^{+7}$ can be more abundant, showing that the solar wind came from a hotter corona. Examples of this are shown in the original Vela 3 report [fig. 1 of *Bame et al.*, 1968*a*], and it has been argued by *Hundhausen et al.* [1968] that these particular examples are obtained in an solar wind stream coming from a single large plage region on the sun [*Hundhausen*, 1970].

A prominent peak at an E/Q four times that of $^{1}H^{+}$ in figure 15 has been attributed to $^{4}He^{+}$. As discussed earlier, almost no $^{4}He^{+}$ is expected to survive in the corona and in the solar wind. However, because of the similar ratio of *A/C* counts in this peak compared to the $^{4}He^{+2}$ peak, it is believed that significant amounts of $^{4}He^{+}$ were present in the solar wind at this time. The ratio $^{4}He^{+}/^{4}He^{+2}$ appeared to be about 3×10^{-3}. Most of the time a peak in this position is not found and upper limits as low as 2×10^{-4} have been set. Based on the identification of $^{4}He^{+}$ in the solar wind, *Hundhausen et al.* [1968] suggested charge exchange of $^{4}He^{+2}$ with interplanetary neutral hydrogen as a source. *Holzer and Axford* [1970*b*] have suggested the ions may result from photoionization of interstellar helium atoms which have penetrated interplanetary space. The infrequent appearance of the peak in the $^{4}He^{+}$ position is not readily explained by either of these mechanisma, and as will be shown later, the $^{4}He^{+}$ identification cannot be made with certainty at the present time.

The group at 2.5 kV was identified as $^{16}O^{+5}$. As

discussed earlier, very little of this species is expected to survive in the solar wind, and its presence was considered anomalous [*Hundhausen et al.*, 1968]. It has been suggested by *Lange and Scherb* [1970] and *Holzer and Axford* [1970*a*] that the counts in this group might be due to $^{28}Si^{+9}$ and $^{32}S^{+10}$; such identifications would avoid the difficulty with $^{16}O^{+5}$. As will be shown later this group is almost certain to consist mainly of $^{28}Si^{+9}$ on the basis of Vela 5 measurements.

The counts in the *A* spectrum of figure 15 above 3.5 kV are very near to the instrumental background at level *A* (shown by the dashed curve). However, the instrumental background at level *C* is very low and it was felt that the *C* counts above 3.5 kV were caused by ions that could not be resolved because of the small numbers of counts and widely spaced levels. The significance of these counts can be judged by reference to table 3 of *Holzer and Axford* [1970*a*], which shows a matrix of *C* counts obtained shortly after the figure 15 data. Holzer and Axford correctly suggested iron ions caused these counts.

Inspection of spectra such as those in figure 15 and other Vela 3 spectra made it clear that the Vela 3 analyzer did not have sufficient efficiency, and that although the intrinsic analyzer efficiency might be adequate, the spacing of E/Q levels was marginal for resolving heavy ion species. A new instrument was designed to be carried on the Vela 5 and 6 satellites. This instrument and measurements from it [*Bame et al.*, 1970] are discussed below, followed by an interpretation of the spectrum of figure 15 in light of the newer measurements from Vela 5A.

Vela 5 and 6 Instrumentation

Each of the four Vela 5 and 6 earth-oriented satellites launched into circular orbits at 20 R_e in May 1969 and April 1970 carries a pair of hemispherical electrostatic analyzers similar to analyzers carried on previous Vela satellites. Particles are analyzed with the sweeping voltage technique and counted in electron multipliers. Each satellite carries one analyzer for standard solar wind measurements, similar to the Vela 4 analyzers described in *Montgomery et al.* [1970]. The second instrument on each satellite has an aperture about three times larger than that of the first and is operated in two modes, which result in considerably higher efficiency for studies of low flux phenomena, including the heavy ion groups found with Vela 3 analyzers.

In the heavy ion operating mode, measurements are made in a total E/Q range from 8000 to 1000 V, which is divided into four separate ranges 1, 2, 3, and 4. Analyzed ions are counted with an electron multiplier and amplifier system having two discrimination levels *A* and *B*; level *B* is 40 times less sensitive than *A*. As with Vela 3, all ions are counted with near 100 percent efficiency at level *A* and considerably less efficiently at *B* for lighter ions.

Spectra of *A* and *B* counts consisting of counts in 80 E/Q levels are measured in an 8.5-min cycle on the Vela 5 and 6 spacecraft, which rotate once every 64 sec. These data are obtained in one of the two operating modes, which can be changed from the ground. As a cycle begins, a sun sensor initiates a series of 25 energy sweeps in E/Q range 1. These sweeps continue over a 5-sec period (~28°), which includes the solar direction in the center. Each sweep is divided into 20 contiguous counting intervals of 8 msec each. The 20 numbers obtained in a single sweep are retained in a memory, numbers from successive sweeps in a given counting interval are added throughout the 25 sweeps, and the totals are transmitted to the ground. In range 1, during the first rotation past the sun, *A* counts are measured. During the second rotation, *B* counts are measured, still in range 1. Range 2 is used, first for *A* counts and next for *B* counts, during the third and fourth revolutions, and so on throughout a complete cycle of eight revolutions.

A complete cycle produces *A*- and *B*-count spectra integrated over angle. Instrumental resolution varies depending on the orientation of the earth-oriented spacecraft. For measurements reported in *Bame et al.* [1970] and discussed here the resolution was ~4.5 percent; the contiguous energy intervals are separated by 2.6 percent, so there are no energy gaps except for small gaps between the sweep ranges. The geometrical angular resolution, also a variable with spacecraft orientation, was ~5°; sweeps are separated by ~1.1°, so there are no gaps in angle. Overall efficiency is increased by making a number of sweeps through the solar wind beam near the direction of peak flux intensity.

The number of usable sets of heavy ion data ultimately obtained from the Vela 5 and 6 heavy ion analyzers will be limited by a number of factors. Among these are the requirements for low ion temperatures, steady solar wind, absence of bow shock generated protons [*Asbridge, et al.*, 1968], proper orientation of the spacecraft roll axis, and that the spacecraft be in the solar wind, in the proper operating mode, and in the active transmitting mode. Vela satellites spend a large fraction of the time in a special memory mode, which does not have the capacity to store heavy ion data.

Vela 5A Heavy Ion Observations

On July 6, 1969, there were several periods of time when bow shock generated protons were not present at the spacecraft and heavy ion measurements could be

made. During these times a clearly delineated $^{16}O^{+6}$ group was observed with a number of smaller peaks occurring at higher values of E/Q. Although the numbers of counts in the smaller peaks were low, the peaks were observed in successive sets of data. Examples are shown in figure 1 of *Bame et al.* [1970]. One of these examples of heavy ion data, combined with a solar wind spectrum integrated over angle, is shown in figure 16. Triangles represent the solar wind spectrum, which was somewhat similar in appearance to the Vela 3 spectrum in figure 14. The heavy ion spectrum (round points) was joined onto the solar wind spectrum by shifting it vertically to overlay the high-energy tail of the $^{4}He^{+2}$ distribution present in both sets of data. Solar wind analyzer counts per sample are given by the left ordinate, and heavy ion counts on the right. The E/Q scale established by the $^{1}H^{+}$ and $^{4}He^{+2}$ peak positions is used to show the expected positions of other ion species; the points in these ion groups have been fitted with 6 percent FWHM gaussian curves, which provide a good fit to the data. Such a width is near enough to the experimental width to show that in this case, the actual E/Q widths of the ion species were less than experimental and undeterminable. However, the $^{1}H^{+}$ and $^{4}He^{+2}$ widths were greater than experimental.

Lines of $^{56}Fe^{+8}$ through $^{56}Fe^{+12}$ are clearly present in this example ($^{56}Fe^{+7}$ has been observed also). Three lines between $^{16}O^{+6}$ and the iron lines could be silicon or sulfur ions within the accuracy of the measurement (table 5 and fig. 13). If the coronal abundances of table 3 are fairly accurate, most of these ions are $^{28}Si^{+9}$, $^{28}Si^{+8}$, and $^{28}Si^{+7}$. Note that $^{28}Si^{+7}$ occupies the expected position of $^{4}He^{+}$, but in this case the A/B counts ratio indicates ions heavier than $^{4}He^{+}$. The argument for the silicon identification of all three lines is strengthened later.

Comparison of figures 16 and 13 shows a remarkable resemblance between the measured and predicted spectra. Part of the resemblance is due to the choice of the $^{4}He^{+2}$ experimental distribution for the prediction and the use of 6 percent line widths in the prediction. However, it is clear that the abundances in table 3 for the photosphere, solar system, and solar cosmic rays would not provide predictions nearly so close to the

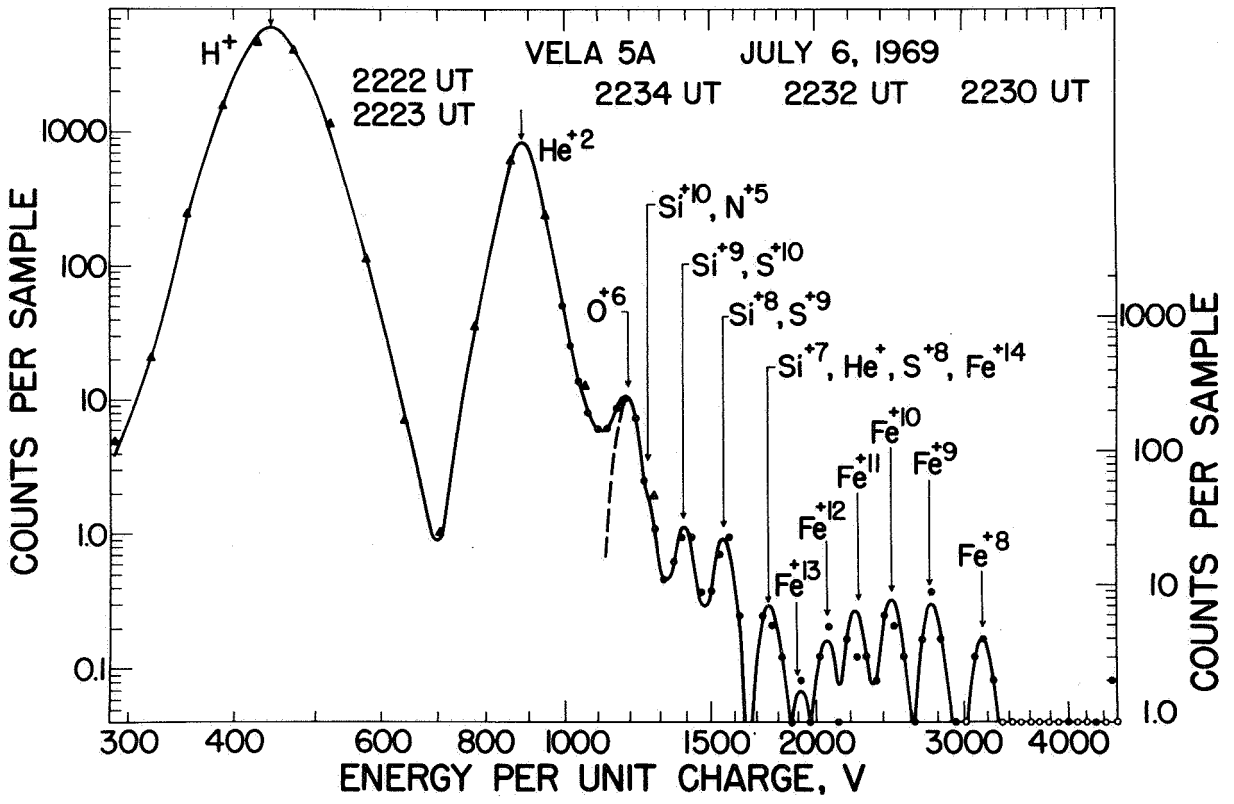

Figure 16. *Combined spectra from the Vela 5A solar wind analyzer and heavy ion analyzer [Bame et al., 1970]. Arrows show the expected positions of various ion groups above $^{16}O^{+6}$. Iron lines are unambiguously resolved and various arguments allow the other three lines above $^{16}O^{+6}$ to be identified as principally silicon ion species.*

measured spectrum at this time. Producing a predicted spectrum in this manner provides insight into which ion species, such as those of sulfur and magnesium, can be expected to be hidden under the lines of the more abundant species; the extent to which these hidden lines contaminate the resolved lines can also be estimated.

One feature in the prediction not appearing in the data is the poorly resolved peak due to $^{12}C^{+5}$. The absence of this peak in the experimental data could be caused by a carbon coronal abundance determination that is too high, an unusually low abundance of carbon in this particular sample of solar wind, or an inaccurate ionization state prediction. If the *Hundhausen et al.* [1968] abundance of ~4 percent $^{12}C^{+5}$ and 96 percent $^{12}C^{+6}$, rather than the 15 percent $^{12}C^{+5}$ value, were used in the prediction, most of the carbon peak would disappear.

Ionization State Coronal Temperatures from Iron Ion Species Abundances. As discussed earlier, solar wind relative abundances freeze in near the sun, and provide information on coronal temperatures. Three heavy ion spectra, including the one in figure 16, were combined to provide better statistics. Because the solar wind speed shifted from 296 to 285 km sec^{-1} during the measurements, small shifts of the E/Q scales were necessary to obtain the best alinement of the groups. The summed spectrum is shown in figure 17. Because of a gap in E/Q coverage between adjacent sweeps, the line attributed to $^{28}Si^{+7}$ in figure 16 was not covered in the succeeding two spectra, after the decrease in speed, so that line is missing in the summed spectrum.

The iron lines, $^{56}Fe^{+8}$ through $^{56}Fe^{+12}$, are clearly resolved here. Because there are no gaps in energy-angle

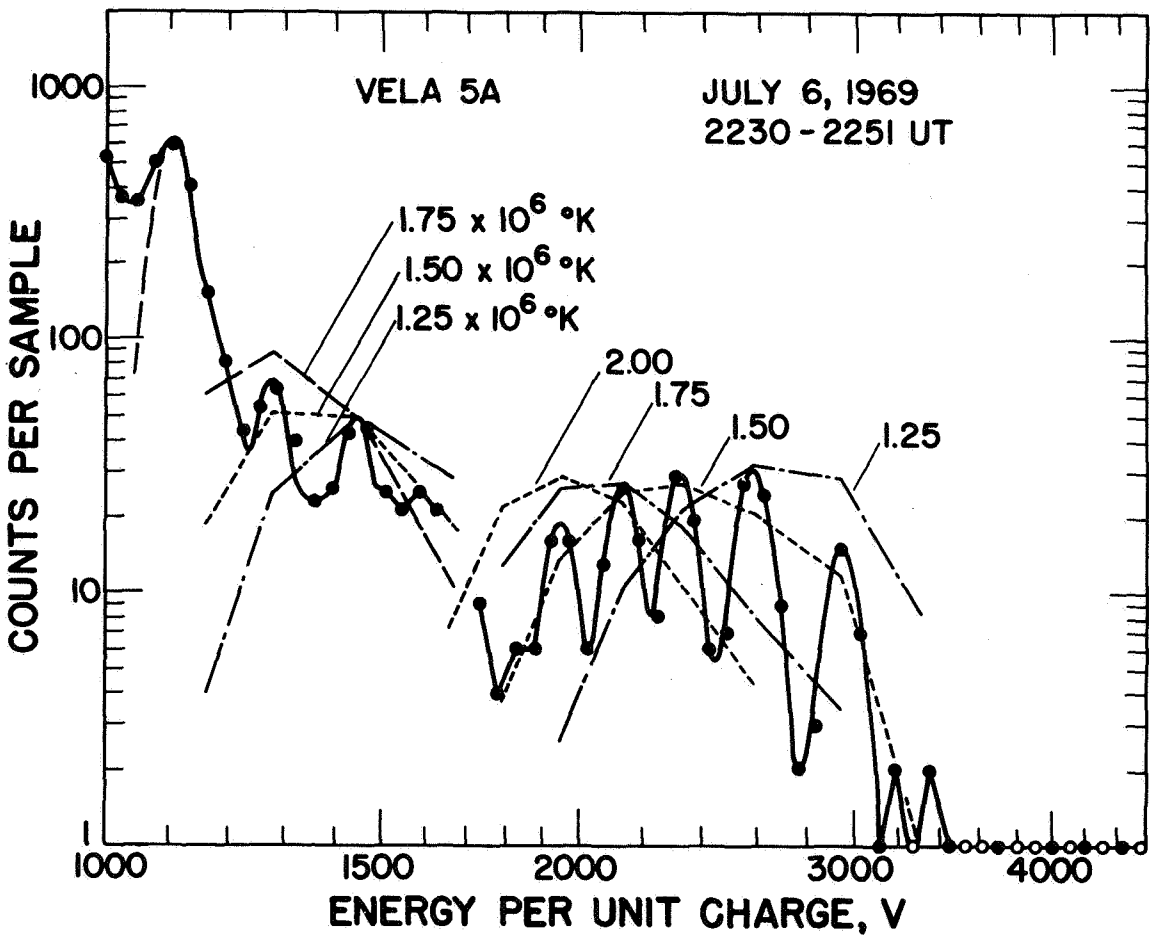

Figure 17. *Vela 5A summed heavy ion spectra [Bame et al., 1970]. Ionization state envelopes from Allen and Dupree [1969] at various temperatures for* ^{56}Fe *and* ^{28}Si *are shown. The iron ion species abundance shows that the temperature of the corona in which this state was determined (frozen-in) was near* 1.5×10^6 °K. *A value* 0.25×10^6 °K *lower is obtained using the results of Jordan [1969].*

coverage and the analyzer resolution is wider than the ion species widths, the peak heights in figure 17 can be used to judge the relative ion abundances for iron. Envelopes of the iron lines for various coronal temperatures, based on calculations by *Allen and Dupree* [1969] are shown. Similar envelopes are obtained with the calculations of *Jordan* [1969] for temperatures about 0.25×10^6°K lower. The iron envelope for 1.5×10^6°K (*A* and *D*) or 1.25×10^6°K(*J*) provides a good fit, but the experimental envelope is broader.

A broader experimental envelope is expected for the expanding corona because the ionization and recombination rates for the various ion species of an element are not the same, and abundance ratios of adjacent species freeze in at different altitudes in the corona. The negative radial temperature gradient in the corona causes the solar wind iron ionization state envelope to be broader than is predicted by the single temperature ionization equilibrium calculations.

Comparison of the ionization and recombination rates and the expansion scale time in the *Whang and Chang* [1965] model corona give about $2R_\odot$ as the heliocentric distance at which the $^{56}Fe^{+12}/^{56}Fe^{+11}$ ratio freezes in and $3R_\odot$ for $^{56}Fe^{+9}/^{56}Fe^{+8}$. (These estimates are from A. J. Hundhausen.) From the data of figure 17, estimates of coronal temperatures for this sample of expanding corona are 1.65×10^6°K at $2R_\odot$ and 1.50×10^6°K at $3R_\odot$ (ionization state calculations of *Allen and Dupree* [1969]). Values about 0.25×10^6°K lower are obtained using the calculations of *Jordan* [1969]. Inspection of the numbers of counts in the iron lines shows that the precision of these temperature estimates is not great.

Identification of Silicon Lines. From table 5 E/Q values, it is apparent that the lines between those of iron and $^{16}O^{+6}$ in figures 16 and 17 conceivably could be caused by either sulfur or silicon. There is no doubt that both elements are present in the solar wind. The lines are identified as principally silicon for the following reasons:

1. $^{28}Si^{+9}$ and $^{32}S^{+10}$ have the greatest separation. The E/Q positions determined in a number of examples, such as figure 18, favor silicon.
2. The measured abundance of iron, discussed later, is similar to the coronal abundance shown in table 3 [*Pottasch*, 1967]. The table shows silicon as almost three times more abundant than sulfur in the corona.
3. The figure 17 ratio of the lines identified as $^{28}Si^{+9}$ and $^{28}Si^{+8}$ gives a temperature of 1.65×10^6°K (*A* and *D*), which compares well with the determinations from the iron lines.
4. The calculations of *Jordan* [1969] include iron, silicon, and sulfur. Comparisons of the calculated and experimental ionization states for $T = 1.26\times10^6$°K are shown in table 6. The experimental iron state comes from figure 17 and seems to agree adequately with the calculated state, showing that about the right temperature (for the calculations of Jordan) has been chosen. Ratios of the three lines in question in figures 16 and 17 are normalized at $^{28}Si^{+8}$ and $^{32}S^{+9}$ in the table to give the experimental states for

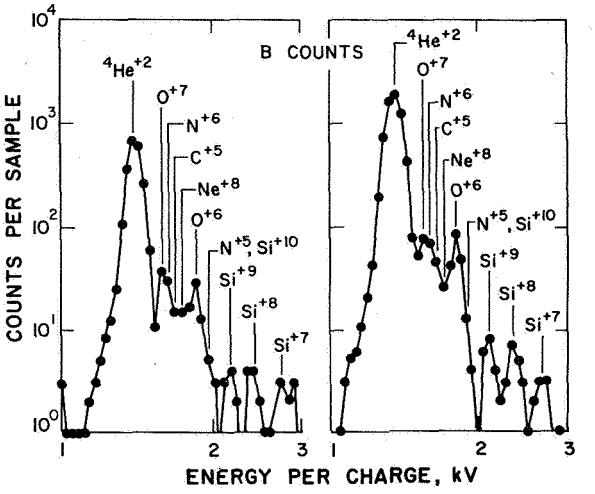

Figure 18. *Two Vela 5A heavy ion spectra. In each, a peak attributed to $^{16}O^{+7}$ and $^{14}N^{+6}$ ions appears between the $^4He^{+2}$ and $^{16}O^{+6}$ peaks. Other ion species, such as $^{12}C^{+5}$, $^{20}Ne^{+8}$, $^{14}N^{+5}$, and $^{28}Si^{+10}$ are also present but unresolved. The E/Q position of the peak identified as $^{28}Si^{+9}$ favors that identification over $^{32}S^{+10}$.*

Table 6 *Comparison of calculated and experimental ionization states of iron, silicon, and sulfur*

	Calculated	Experimental
Fe^{+7}	0.01	--
Fe^{+8}	.08	0.12
Fe^{+9}	.23	.25
Fe^{+10}	.31	.24
Fe^{+11}	.23	.21
Fe^{+12}	.12	.14
Fe^{+13}	.02	--
Si^{+7}	.09	.11
Si^{+8}	.31	(.31)
Si^{+9}	.44	.41
Si^{+10}	.14	--
S^{+8}	.31	.14
S^{+9}	.43	(.43)
S^{+10}	.16	.55

silicon and sulfur. Comparison of these states with the calculated states clearly favors the silicon identification.

Presence of $^{16}O^{+7}$ *and* $^{14}N^{+6}$ *Ions.* Observations from Vela 3 have been interpreted in the past as showing cases when $^{16}O^{+7}$ was more abundant than $^{16}O^{+6}$. Such an observation depended on chance alinement of levels near the expected ion species positions; inadequate numbers of levels prevented complete resolution of the experimental spectra. Vela 5 and 6 heavy ion measurements provide considerably better coverage, and in one case investigated thus far, the $^{4}He^{+2}$ temperature was low enough to permit resolution of structure between $^{4}He^{+2}$ and $^{16}O^{+6}$.

Vela 5A data taken June 22, 1969, at 2100 UT and June 23, 1969, at 0450 UT are shown in figure 18. Note that *B*-count spectra better separate heavier ions in the $^{4}He^{+2}$ high-energy tail. Similar spectra were measured throughout the time span of these spectra. Lines show the expected positions (table 5) of various ion species based on the helium position. The presence of $^{16}O^{+7}$ along with some $^{14}N^{+6}$ in this solar wind sample seems well established. Smaller amounts of $^{12}C^{+5}$ and $^{20}Ne^{+8}$ are undoubtedly also present but not resolved. $^{14}N^{+5}$ and $^{28}Si^{+10}$ ions contribute to the high-energy tail of the $^{16}O^{+6}$ peak, but are not resolved. The three prominent silicon lines indicate that this solar wind came from a corona at temperatures near 1.5×10^{6}°K, or 1.25×10^{6}°K depending on the choice of ionization state calculations. Relative abundances should not be estimated from these spectra because the *B*-counts response to various species is not known accurately. Relative abundance estimates of oxygen, silicon, and iron from this time, using the near 100 percent response of the *A*-count spectra, are about the same as those estimated from figures 16 and 17.

Reinterpretation of Vela 3 Spectra and the $^{4}He^{+}$ Problem

Spectra from Vela 3 can be reinterpreted on the basis of the more adequate sensitivity and E/Q coverage of the Vela 5A measurements. Figure 19 shows the Vela 3A spectrum given in figure 15; here the *A*-count points are fitted with a spectrum that draws on the Vela 5A results shown in figures 16, 17, and 18. The peak originally identified as $^{16}O^{+5}$ can now be identified as $^{28}Si^{+9}$, eliminating the difficulties with the oxygen identification pointed out by *Hundhausen et al.* [1968], *Lange and Scherb* [1970], and *Holzer and Axford* [1970*a*]. The iron ion species peaks have no real significance other than to demonstrate the presence of iron ions above the background level; wide separations of the

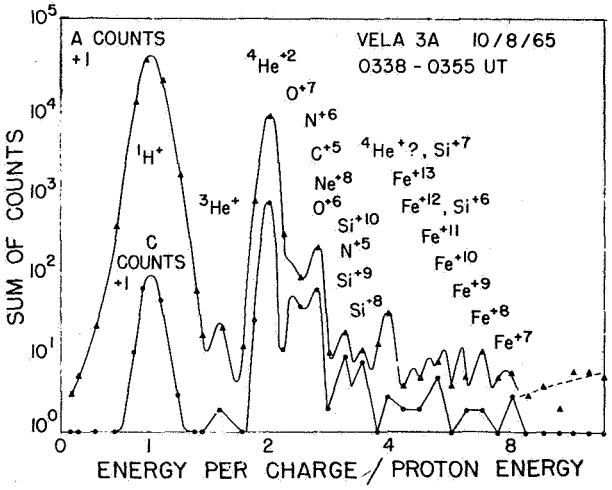

Figure 19. *A Vela 3A spectrum (also shown in fig. 15) with identifications based on the more recent Vela 5A results. The multiple peaks drawn in the* ^{56}Fe *ion positions are meant to show only that the experimental points are consistent with the presence of unresolved lines above background. The peak at 4.0 is anomalously high to be explained as due only to* $^{28}Si^{+7}$ *ions.*

Vela 3 E/Q levels and low sensitivity prevented resolution of individual lines.

In this case, E/Q levels fortunately fell near the silicon peak positions. It is difficult to reconcile the relative heights of the peaks to any reasonable ionization state of silicon. For this reason, there appears to be a significant excess of counts at the position of $^{28}Si^{+7}$, which is also the position of $^{4}He^{+}$. The *A*/*C* counts ratio at that position, although statistically not too accurate, suggests that helium-like ions might be present (compare *A*/*C* ratios at the $^{28}Si^{+9}$ and $^{28}Si^{+8}$ positions). Finally, the Si/O ratio from this spectrum would be high compared to Vela 5A results, if all the ions are taken to be $^{28}Si^{+7}$ in the peak. If great differences occur in differentiation of elements in the corona, it is possible that this E/Q position at four times the $^{1}H^{+}$ position might indicate an enhanced flux caused by $^{28}Si^{+7}$, $^{32}S^{+8}$, and $^{36}Ar^{+9}$ ions coming from a relatively cool location in the corona.

The identification of $^{4}He^{+}$ in the solar wind [*Bame et al.*, 1968*a*] was based on three cases in which a peak occurred in the $E/Q = 4.0$ position. Figure 19 was one of the cases. Usually such peaks are absent in Vela 3 data. All three spectra with identifiable peaks are shown in figure 20, and in each example the prominent line at 4.0

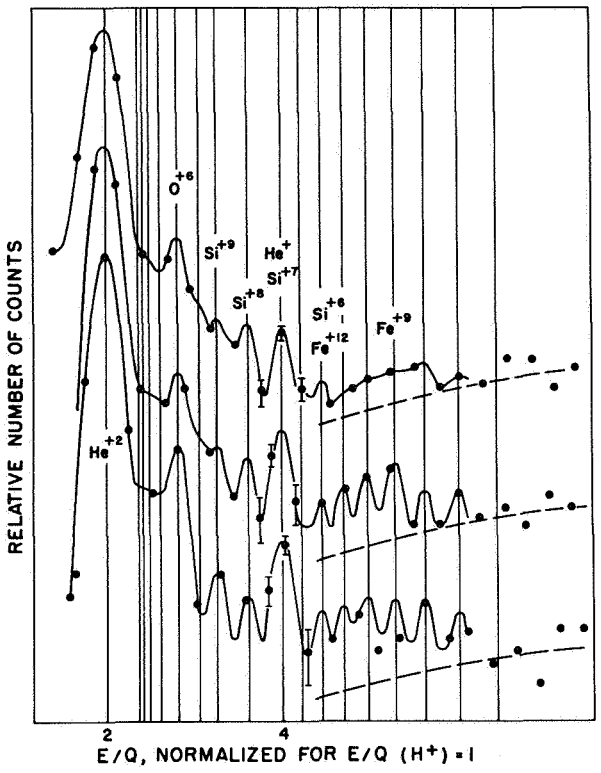

Figure 20. *Three Vela 3 spectra with prominent peaks in the E/Q = 4.0 positions. Vertical lines give the positions of various ion species which are expected to be present. Multiple peaks drawn through the points at the* ^{56}Fe *species positions are symbolic only.*

appears accentuated compared to the $^{16}O^{+6}$ peaks of the Vela 5A data shown in figure 18. However, in two cases, points do not lie near the peaks of the $^{16}O^{+6}$, $^{28}Si^{+9}$, and $^{28}Si^{+8}$ positions, so the argument for $^{4}He^{+}$ is not so strong as in the case shown in figure 19.

Whether or not $^{4}He^{+}$ ions occasionally are present in the solar wind remains an open question. If they are, the higher sensitivity and better spectral resolution of the Vela 5 and 6 heavy ion analyzers should make possible a more definite identification, if $^{4}He^{+}$ should appear during periods of measurements.

Solar Wind Composition

The Vela 5A spectra in figures 16 and 17 have been used to derive the abundances for the July 6, 1969, solar wind. For this sample, oxygen, silicon, and iron abundances are estimated from figure 17 data using relative peak heights. Hydrogen and helium abundances are estimated using the figure 16 data and taking into account the peak widths. It is assumed that peak heights are not seriously contaminated with unresolved species. In the synthesized spectrum of figure 13, the maximum contamination in a resolved peak height was 20 percent for $^{28}Si^{+9}$. The $^{16}O^{+6}$ peak height was contaminated by 10 percent. Oxygen is assumed to be 17 percent $^{16}O^{+7}$ and 83 percent $^{16}O^{+6}$. Figure 16 is used to estimate $^{28}Si^{+7}$ and the same amount of $^{28}Si^{+10}$ is assumed. From these assumptions the relative abundances of hydrogen, helium, oxygen, silicon, and iron are found to be 5000, 150, 1.00, 0.21, and 0.17. The silicon and iron abundances relative to oxygen compare well with the table 3 coronal abundances. The uncertainty in these abundances is thought to be about ±30 percent.

Table 7 summarizes the ion species identified in the solar wind. Whether or not $^{4}He^{+}$ ever appears seems to be an open question. There seems to be no doubt that such species as $^{12}C^{+5}$, $^{20}Ne^{+8}$, $^{24}Mg^{+10}$, $^{14}N^{+5}$, $^{32}S^{+9}$, and $^{32}S^{+10}$ are also carried in the solar wind. Ions of other less abundant coronal elements such as calcium and nickel must also be present, but may not be identified for some time to come.

Table 8 lists the elements and isotopes detected in the solar wind by means of spacecraft observations and the lunar collector foil technique used by *Bühler et al.* [1969] and *Geiss et al.* [1970*b*]. Again it should be pointed out that the elements and isotopes known to be present in the corona should also be present in the solar wind, but not all of them have yet been identified.

Table 9 summarizes relative abundances of heavier ions in the corona and solar wind. The values of *Pottasch* [1967] are used for the corona. Values of solar wind abundances for oxygen, silicon, and iron come from the Vela 5A data of July 6, 1969. A few other samples of Vela 5 data have shown similar O-Si-Fe ratios, but a greater sample of data must be studied before it is clear how constant these ratios may be. The abundances of the other common elements, such as carbon, nitrogen, and sulfur, in the solar wind remain to be determined since they are not sufficiently resolved in the Vela data. The abundance given for ^{20}Ne has been estimated by *Geiss et al.* [1970*b*] on the basis of the Apollo foil experiments and the Vela 3 measurements of He/O ratios.

Estimates of He/O from Vela range from around 30 to over 400. There is no doubt about the variability of this ratio; the average may be near 100. The helium-hydrogen ratio is variable over a range of two orders of magnitude, and has a well established average near 0.045. The $^{3}He/^{4}He$ ratio measured by Vela also is variable; an upper limit as low as 2×10^{-4} has been observed, while on other occasions the ratio exceeds 10^{-3}. *Geiss et al.* [1970*b*] have observed $^{3}He/^{4}He$ ratios

of $5.4X10^{-4}$ and $4.1X10^{-4}$ from the Apollo 11 and 12 solar wind experiments. These authors consider the variation to be real.

The temperatures of ion species above $^4He^{+2}$ cannot be determined from the Vela 5 data given here, because of the narrow E/Q widths. It is clear that the temperatures are lower than the ratios of masses of the heavier ions to hydrogen multiplied by the hydrogen temperature. In Vela 3 examples, directional distributions were also determined, from which transverse temperatures can be estimated. Again, heavier ions appear to generally have lower temperatures than the ratios of masses times the hydrogen temperature, but the accuracy of the result is limited by the fact that experimental widths are close to instrumental widths.

Table 7 *Ion species identified in solar wind*

$^1H^+$	Mariner 2, two groups in E/Q spectrum
$^4He^{+2}$	Vela 3, second group higher mass Explorer 34, M/Q analysis
$^3He^{+2}$	Vela 3, E/Q spectrum
$^4He^+$?	
$^{14}N^{+6}$	Vela 5, E/Q spectrum
$^{16}O^{+6}$–$^{16}O^{+7}$	Vela 3, E/Q spectrum
$^{28}Si^{+7}$–$^{28}Si^{+9}$	Vela 5, E/Q spectrum
$^{56}Fe^{+7}$–$^{56}Fe^{+12}$	

Table 8 *Elements and isotopes identified in the solar wind*

^1H	Mariner 2, two groups in E/Q spectrum Vela 3, second group higher mass Explorer 34, M/Q analysis Apollo foil (mass spectrometer)
^4He	
^3He	Vela 3 E/Q spectrum, Apollo foil
^{14}N	Vela 5 E/Q spectrum
^{16}O	Vela 3 E/Q spectrum
^{20}Ne	Apollo foil, mass spectrometer
^{21}Ne	
^{22}Ne	
^{28}Si	Vela 5 E/Q spectrum
^{56}Fe	

Table 9 *Corona and solar wind relative abundances*

	Corona abundance	Solar wind abundance
^{12}C	2.00	--
^{14}N	.24	--
^{16}O	1.00	1.00
^{20}Ne	.14	.1
^{24}Mg	.12	--
^{28}Si	.20	.21
^{32}S	.08	--
^{56}Fe	.20	.17

ACKNOWLEDGMENTS

The author wishes to thank Drs. J. R. Asbridge, A. J. Hundhausen, and M. D. Montgomery for discussions pertinent to this review. The assistance of Dr. P. D. Kearney of Colorado State University with some of the previously unpublished Vela data is gratefully acknowledged. The Vela portions of data presented here were obtained from the Vela nuclear test detection satellites that have been designed, developed and flown as a part of a joint program of the Advanced Research Projects Agency of the U.S. Department of Defense and the U.S. Atomic Energy Commission. The program is managed by the U.S. Air Force.

REFERENCES

Allen, C. W.: *Astrophysical Quantities 30-1,* Athlone Press, Univ. London, London, England, 1963.

Allen, J. W.; and Dupree, A. K.: Calculations of Ionization Equilibria for Oxygen, Neon, Silicon, and Iron. *Astrophys. J.,* Vol. 155, 1969, p. 27.

Asbridge, J. R.; Bame, S. J.; and Strong, I. B.: Outward Flow of Protons from the Earth's Bow Shock. *J. Geophys. Res.,* Vol. 73, 1968, p. 5777.

Bame, S. J.; Asbridge, J. R.; Felthauser, H. E.; Hones, E. W.; and Strong, I. B.: Characteristics of the Plasma Sheet in the Earth's Magnetotail. *J. Geophys. Res.,* Vol. 72, 1967, p. 113.

Bame, S. J.; Hundhausen, A. J.; Asbridge, J. R.; and Strong, I. B.: Solar Wind Ion Composition. *Phys. Rev. Lett.,* Vol. 20, 1968*a*, p. 393.

Bame, S. J.; Asbridge, J. R.; Hundhausen, A. J.; and Strong, I. B.: Solar Wind and Magnetosheath Observations During the Jan. 13-14, 1967, Geomagnetic Storm. *J. Geophys. Res.,* Vol. 73, 1968*b*, p. 5761.

Bame, S. J.; Asbridge, J. R.; Hundhausen, A. J.; and Montgomery, M. D.: Solar Wind Ions: $^{56}Fe^{+8}$ to $^{56}Fe^{+12}$, $^{28}Si^{+7}$, $^{28}Si^{+8}$, $^{28}Si^{+9}$, and $^{16}O^{+6}$. *J. Geophys. Res.,* Vol. 75, 1970, p. 6360.

Baschek, B.; Garz, T.; Richter, J.; and Holweger, H.: Experimentelle Oszillatorenstarken von Fe II-Linien und die Solare Eisenhaufigkeit. *Astron. Astrophys.,* Vol. 4, 1970, p. 229.

Bertsch, D. L.; Fichtel, C. E.; and Reames, D. V.: Relative Abundance of Iron-Group Nuclei in Solar Cosmic Rays. *Astrophys. J.*, Vol. 157, 1969, p. L53.

Biswas, S.; Fichtel, C. E.; and Guss, D. E.: Solar Cosmic Ray Multiply Charged Nuclei and the July 18, 1961, Solar Event. *J. Geophys. Res.*, Vol. 71, 1966, p. 4071.

Bühler, F.; Eberhardt, P.; Geiss, J.; and Meister, J.: Apollo 11 Solar Wind Composition Experiment: First Results. *Science*, Vol. 166, 1969, p. 1502.

Cameron, A. G. W.: A New Table of Abundance of the Elements in the Solar System. *Origin and Distribution of the Elements*, edited by L. H. Ahrens, Pergamon Press, New York, 1968, pp. 125-143.

Cummings, W. D.; and Coleman, P. J., Jr.: Magnetic Fields in the Magnetopause and Vicinity at Synchronous Altitude. *J. Geophys. Res.*, Vol. 73, 1968, p. 5699.

Coon, J. H.: Vela Satellite Measurements of Particles in the Solar Wind and the Distant Geomagnetosphere. *Radiation Trapped in the Earth's Magnetic Field*, edited by B. M. McCormac, D. Reidel, New York, 1966, p. 231.

Cox, D. P.; and Tucker, W. H.: Ionization Equilibrium and Radiative Cooling of a Low Density Plasma. *Astrophys. J.*, Vol. 157, 1969, p. 1157.

Davis, R., Jr.; Harmer, D. S.; and Hoffman, K. C.: Search for Neutrinos From the Sun. *Phys. Rev. Lett.*, Vol. 20, 1968, p. 1205.

Demarque, P. R.; and Percy, J. R.: A Series of Solar Models. *Astrophys. J.*, Vol. 140, 1964, p. 541.

Durgaprasad, N.; Fichtel, C. E.; Guss, D. E.; and Reames, D. V.: Nuclear-Charge Spectra and Energy Spectra in the Sept. 2, 1966, Solar-Particle Event. *Astrophys. J.*, Vol. 154, 1968, p. 307.

Fedoretz, V. A.; and Ezerskii, V. N.: *Circ. Kharkov. Obs.*, Vol. 18, 1953, p. 10.

Formisano, V.; Palmiotto, F.; and Moreno, G.: α-Particle Observations in the Solar Wind. *Solar Phys.*, Vol. 15, 1970, p. 479.

Garz, T.; Holweger, H.; Kock, M.; and Richter, J.: Revision der solaren eisenhaufigkeit und ihre bedeutung das modell der sonnenphotosphare. *Astron. Astrophys.*, Vol. 2, 1969*a*, p. 446.

Garz, T.; Kock, M.; Richter, J.; Baschek, B.; Holweger, H.; and Unsöld, A.: Abundances of Iron and Some Other Elements in the Sun and in Meteorites. *Nature*, Vol. 223, 1969*b*, p. 1254.

Gaustad, J. E.: The Solar Helium Abundance. *Astrophys. J.*, Vol. 139, 1964, p. 406.

Geiss, J.; Hirt, P.; and Lentwyler, H.: On Acceleration and Motion of Ions in Corona and Solar Wind. *Solar Phys.*, Vol. 13, 1970*a*, p. 183.

Geiss, J.; Eberhardt, P.; Buhler, F.; Meister, J.; and Signer, P.: Apollo 11 and 12 Solar Wind Composition Experiments: Fluxes of He and Ne Isotopes. *J. Geophys. Res.*, Vol. 75, 1970*b*, p. 5972.

Goldberg, L.; Müller, E. A.; and Aller, L. H.: The Abundances of the Elements in the Solar Atmosphere. *Astrophys. J. Supp.*, Vol. 5, 1960, p. 1.

Gosling, J. T.; Asbridge, J. R.; Bame, S. J.; and Strong, I. B.: Vela 2 Measurements of the Magnetopause and Bow Shock Positions. *J. Geophys. Res.*, Vol. 72, 1967*a*, p. 101.

Gosling, J. T.; Asbridge, J. R.; Bame, S. J.; Hundhausen, A. J.; and Strong, I. B.: Measurements of the Interplanetary Solar Wind During the Large Geomagnetic Storm of April 17-18, 1965. *J. Geophys. Res.*, Vol. 72, 1967*b*, p. 1813.

Grevesse, N.: Ph.D. Thesis, Liege, 1969.

Grevesse, N.; and Swings, J. P.: Forbidden Lines of Fe II in the Solar Photospheric Spectrum. *Astron. Astrophys.*, Vol. 2, 1969, p. 28.

Hirshberg, J.; Alksne, A.; Colburn, D. S.; Bame, S. J.; and Hundhausen, A. J.: Observation of a Solar-Flare-Induced Interplanetary Shock and Helium-Enriched Driver Gas. *J. Geophys. Res.*, Vol. 75, 1970*a*, p. 1.

Hirshberg, J.; Bame, S. J.; and Robbins, D. E.: Helium Enriched Interplanetary Medium and Solar Flares. *Trans. Amer. Geophys. Union.* Vol. 51, 1970*b*, p. 818.

Holzer, T. E.; and Axford, W. I.: Solar Wind Ion Composition. *J. Geophys. Res.*, Vol. 75, 1970*a*, p. 6354.

Holzer, T. E.; and Axford, W. I: He^+ Ions in the Solar Wind. *Trans. Amer. Geophys. Union*, Vol. 51, 1970*b*, p. 411.

Hundhausen, A. J.; Asbridge, J. R.; Bame, S. J.; Gilbert, H. E.; and Strong, I. B.: Vela 3 Satellite Observations of Solar Wind Ions: A Preliminary Report. *J. Geophys. Res.*, Vol. 72, 1967, p. 87.

Hundhausen, A. J.; Gilbert, H. E.; and Bame, S. J.: Ionization State of the Interplanetary Plasma. *J. Geophys. Res.*, Vol. 73, 1968, p. 5485.

Hundhausen, A. J.: Composition and Dynamics of the Solar Wind Plasma. *Rev. Geophys. Space Phys.*, Vol. 8, 1970, p. 729.

Iben, Icko, Jr.: The Cl^{37} Solar Neutrino Experiment and the Solar Helium Abundance. *Ann. Phys.*, Vol. 54, 1969, p. 164.

Jordan, C.: The Relative Abundance of Silicon, Iron, and Nickel in the Solar Corona. *Mon. Notic. Roy. Astron. Soc.*, Vol. 132, 1966, p. 463.

Jordan, C.: The Ionization Equilibrium of Elements Between Carbon and Nickel. *Mon. Notic. Roy. Astron. Soc.*, Vol. 142, 1969, p. 501.

Kavanagh, L. D., Jr.; Schardt, A. W.; and Roelof, E. C.: Solar Wind and Solar Energetic Particles: Properties and Interactions. *Rev. Geophys. Space Phys.*, Vol. 8, 1970, p. 389.

Lambert, D. L.: Abundance of Helium in the Sun. *Nature*, Vol. 215, 1967, p. 43.

Lange, J.; and Scherb, F.: Ion Abundances in the Solar Wind. *J. Geophys. Res.*, Vol. 75, 1970, p. 6350.

Lazarus, A. J.; Bridge, H. S.; and Davis, J.: Preliminary Results from the Pioneer 6 MIT Plasma Experiment. *J. Geophys. Res.*, Vol. 71, 1966, p. 3787.

Lazarus, A. J.; and Binsack, J. H.: Observations of the Interplanetary Plasma Subsequent to the July 7, 1966, Proton Flare. *Ann. IQSY*, Vol. 3, 1969, p. 378.

Malville, J. M.; and Schmahl, E. J.: Photoelectric Measurements of the Green Coronal Line During the Eclipse of November 2, 1966. *Solar Phys.*, Vol. 4, 1968, p. 224.

Montgomery, M. D.; Asbridge, J. R.; and Bame, S. J.: Vela 4 Plasma Observations Near the Earth's Bow Shock. *J. Geophys. Res.*, Vol. 75, 1970, p. 1217.

Morton, D. C.: The Abundance of Helium in *A*- and *B*-Type Stars. *Astrophys. J.*, Vol. 151, 1968, p. 285.

Nakada, M. P.: A Study of the Composition of the Solar Corona and Solar Wind. *Solar Phys.*, Vol. 14, 1970, p. 457.

Neugebauer, M.; and Snyder, C. W.: Mariner 2 Observations of the Solar Wind, 1, Average Properties. *J. Geophys. Res.*, Vol. 71, 1966, p. 4469.

Nikolski, G. M.: The Energy Distribution in the Solar EUV Spectrum and Abundance of Elements in the Solar Atmosphere. *Solar Phys.*, Vol. 6, 1969, p. 399.

Nussbaumer, H.; and Swings, J. P.: [Fe II] Magnetic Dipole Transition Probabilities and the Problem of the Solar Iron Abundance. *Astron. Astrophys.*, Vol. 7, 1970, p. 455.

Ogilvie, K. W.; Burlaga, L. F.; and Wilkerson, T. D.: Plasma Observations on Explorer 34. *J. Geophys. Res.*, Vol. 73, 1968*a*, p. 6809.

Ogilvie, K. W.; McIlwraith, N.; and Wilkerson, T. D.: A Mass-Energy Analyzer for Space Plasmas. *Rev. Sci. Instru.*, Vol. 39, 1968*b*, p. 441.

Ogilvie, K. W.; and Wilkerson, T. D.: Helium Abundance in the Solar Wind. *Solar Phys.*, Vol. 8, 1969, p. 435.

Parker, E. N.: Comments on Coronal Heating. *The Solar Corona*, edited by J. W. Evans, Academc Press, New York, 1963.

Pecker, J. C.; and Pottasch, S. R.: On the Abundance Determination in the Solar Chromosphere. *Astron. Astrophys.*, Vol. 2, 1969, p. 81.

Pottasch, S. R.: On the Chemical Composition of the Solar Corona. *Mon. Notic. Royal Astron. Soc.*, Vol. 128, 1964, p. 73.

Pottasch, S. R.: The Inclusion of Dielectronic Recombination Processes in the Interpretation of the Solar Ultraviolet Spectrum. *Bull. Astron. Inst. Neth.*, Vol. 19, 1967, p. 113.

Pottasch, S. R.: *Origin and Distribution of the Elements*, Edited by L. H. Ahrens, Pergamon Press, London, 1968.

Robbins, D. E.; Hundhausen, A. J.; and Bame, S. J.: Helium in the Solar Wind. *J. Geophys. Res.*, Vol. 75, 1970, p. 1178.

Rogerson, J. B.: On the Abundance of Iron in the Solar Photosphere. *Astrophys. J.*, Vol. 158, 1969, p. 797.

Ross, J.: Abundance of Iron in the Solar Photosphere. *Nature*, Vol. 225, 1970, p. 610.

Sears, R. L.: Helium content and Neutrino Fluxes in Solar Models. *Astrophys. J.*, Vol. 140, 1964, p. 477.

Snyder, C. W.; and Neugebauer, M.: Interplanetary Solar Wind Measurements by Mariner 2. *Space Res.*, Vol. 4, 1964, p. 89.

Tucker, W. H.; and Gould, R. J.: Radiation from a Low Density Plasma at 10^6-10^8 °K. *Astrophys. J.*, Vol. 144, 1966, p. 244.

Unsöld, A. O. J.: Stellar Abundances and Origin of Elements. *Science*, Vol. 163, 1969, p. 1015.

Urey, H. C.: The Abundance of the Elements with Special Reference to the Problem of the Iron Abundance. *Quart. J. Roy. Astron. Soc.*, Vol. 8, 1967, p. 23.

Weymann, R.; and Sears, R. L.: The Depth of the Convective Envelope on the Lower Main Sequence and the Depletion of Lithium. *Astrophys. J.*, Vol. 142, 1965, p. 174.

Whang, Y. C.; and Chang, C. C.: An Inviscid Model of the Solar Wind. *J. Geophys. Res.*, Vol. 70, 1965, p. 4175.

Widing, K. G.; and Sandlin, G. D: Analysis of the Solar Spectrum in the Spectral Range 33-110 Å. *Astrophys. J.*, Vol. 152, 1968, p. 545.

Withbroe, G. L.: The Photospheric Abundance of Iron. *Solar Phys.*, Vol. 9, 1969, p. 19.

Wolfe, J. H.; and Silva, R. W.: Explorer 14 Plasma Probe Observations During the Oct. 7, 1962, Geomagnetic Disturbance. *J. Geophys. Res.*, Vol. 70, 1965, p. 3575.

Wolfe, J. H.; Silva, R. W.; McKibbin, D. D.; and Mason, R. H.: The Compositional, Anisotropic, and Non-radial Flow Characteristics of the Solar Wind. *J. Geophys. Res.*, Vol. 71, 1966, p. 3329.

DISCUSSION

B. M. McCormac To what extent did you consider autoionization in your predictions of the various species?

S. J. Bame I believe autoionization was considered by Allen, Dupree, and Jordan in their calculations. I have not made those calculations myself.

B. M. McCormac This should make a substantial difference, particularly in the nitrogen oxygen species.

W. F. Feldman You mentioned that there was one unimpeachable spectrum for helium plus and mentioned in your original paper a density of 3×10^{-3}. Could you quote an error bar?

S. J. Bame I wouldn't want to say it's unimpeachable.

W. F. Feldman Well, you said it couldn't be explained as silicon and it is anomolous.

S. J. Bame We can't explain it as silicon. It kept appearing in successive spectra, so it's very difficult to believe it wasn't there. With respect to the error, I think there was something on the order of about 50 counts in the peak of the sum spectra. So it's not of very high accuracy statistically.

G. E. Thomas Concerning the problem with presence of He^+ in the solar wind, I understand from the publications concerning this that one of the explanations for it was He^{++} charge exchanging with neutral hydrogen.

S. J. Bame Yes.

G. E. Thomas Presumably the neutral hydrogen would come from the intersteller medium, and, as I understand, you noticed a flux of $\sim2\times10^6$ cm^{-2} sec^{-1}. In our Lyman-α scattering measurements of neutral hydrogen it's difficult for us to understand such high fluxes, and we think probably a more realistic number would be 10 to 10^2 times less than that. I think the theoretical support is weak also.

S. J. Bame That is correct. There have been two suggestions as to possible causes of the He^+ peak, one being charge exchange with interstellar hydrogen and the other charge exchange with interplanetary hydrogen. But one of the problems is that neither of these mechanisms, it seems to me, explains the fact that it is there sometimes and other times it is not.

T. E. Holzer We suggest a mechanism by which He^+ from interstellar space is photoionized; I think that that will fit in with your Lyman-α observations.

G. W. Simon You showed a neon value. Is that from Geiss's work?

S. J. Bame Yes, that's Geiss's work. You may recall the last spectrum I showed (fig. 19) where we actually were able to see a little structure between the helium peak and the oxygen peak; the neon is in the valley between the group that we call N^{6+} and O^{7+}. We are just unable to resolve it so I would guess off-hand that the value of 0.1 that Geiss has given for its abundance relative to oxygen is probably reasonable.

J. Geiss When you have a high flux of helium, as in a driver gas, is the oxygen also enhanced relative to the hydrogen?

S. J. Bame I would guess that the answer to that question is yes, but it's a little questionable. Most of the times that we've been able to see the heavy ions have been times when the helium was particularly abundant. I don't think we have looked at many cases in which the helium is not very abundant as we cannot see the heavier ions at those times.